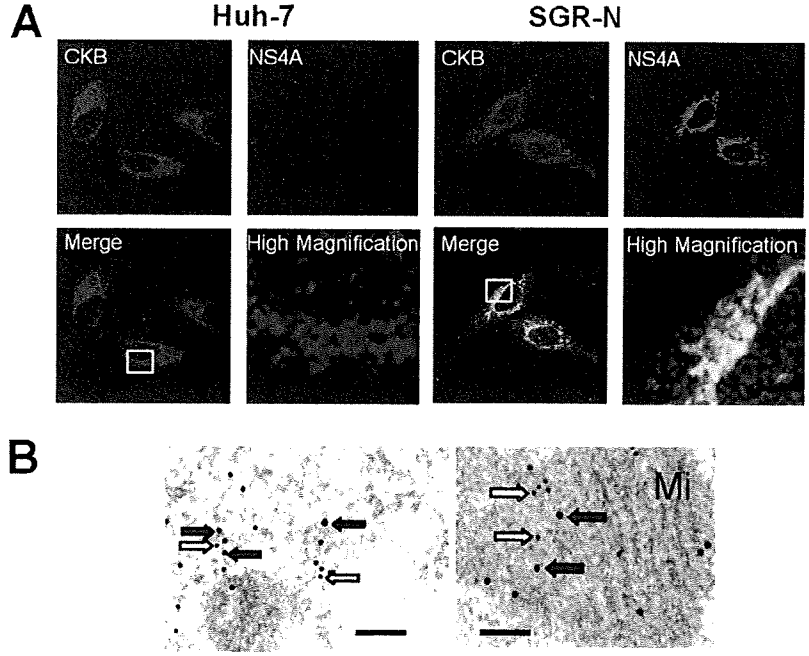

FIG. 4. Colocalization of CKB with HCV NS4A. (A) Indirect immunofluorescence analysis. The primary antibodies used were anti-CKB goat PAb (red) and anti-NS4A MAb (green). Merged images of red and green signals are shown. High-magnification panels are enlarged images of white squares in the merge panels. (B) Immunoelectron microscopic localization of CKB and NS4A. SGR-N cells were double-immunolabeled for CKB (12-nm gold particles; white arrows) and for NS4A (18-nm gold particle; gray arrows). Mi, mitochondria. Bars, 200 nm.

CKB colocalized with NS4A in the cytoplasmic electron-dense regions, presumably derived from altered or folded membrane structures (Fig. 4B, left panel) and mitochondria (Fig. 4B, right panel).

CKB enhances functional HCV replicase and NS3-4A helicase. NS4A is known to mediate membrane association of the NS3-4A complex and to function as a cofactor in NS3 enzyme activity. To understand the mechanism(s) underlying positive regulation of HCV RNA replication through CKB via its interaction with NS4A, we first investigated whether CKB modulates NS3-4A helicase activity. NS3-4A helicase is a member of the superfamily-2 DexH/D-box helicase, which unwinds RNA-RNA substrates in a 3′-to-5′ direction. During RNA replication, the NS3-4A helicase is believed to translocate along the nucleic acid substrate by changing its protein conformation, utilizing the energy of ATP hydrolysis (9). We then tested the effect of CKB on RNA- or DNA-unwinding activity using purified recombinant full-length NS3 and NS3-4A complex (12). As shown in Fig. 5A (left middle panel), both NS3 and NS3-4A helicase activity unwound dsRNA substrate most efficiently when CKB, ATP, and pCr were added to the reaction mixture. The enhancing effect of CKB was observed in the presence of pCr but not in the absence of it, suggesting that catalytic activity of CKB is important for its effect on the HCV helicase activity. Similar results were obtained from the DNA helicase assay using dsDNA substrate (Fig. 5B). To address the specificity of the stimulation by the CKB/pCr system, effects of PK and pPy, which are also involved in the ATP generation, were determined (Fig. 5A, right panels). Exogenous PK and pPy at the same concentrations as those of CKB and pCr used in the study exhibited no effect on the HCV helicase activity.

The effect of CKB on NS3-4A serine protease activity, which is considered to be ATP-independent, was also assessed in an in vitro protease assay using the purified viral proteins as mentioned above (Fig. 5C). As expected, NS3-4A complex exhibited significantly higher activity than NS3 alone; however, CKB did not affect the protease activities of NS3 or NS3-4A.

Finally, we investigated loss and gain of function of CKB in HCV replicase activity, which requires high-energy phosphate, in the context of semi-intact replicon cells. Miyanari et al. (33) reported that the function of the active HCV RC can be monitored in permeabilized replicon cells treated with digitonin. Thus, permeabilized replicon cells in the presence or absence of exogenous CKB were incubated with [α-^{32}P]UTP to detect newly synthesized RNA. As indicated in Fig. 5D, an ~8-kb band corresponding to HCV subgenomic RNA was most abundant in cells in the presence of exogenous CKB, ATP and pCr. The enhancing effect of CKB was observed in the presence but not in the absence of pCr, suggesting that catalytic activity of CKB is important for its effect on the replicase activity. As for the RNA helicase assay, exogenous PK and pPy did not enhance the replicase activity (data not shown). HCV replicase activity in permeabilized cells to which we had introduced siCKB-2 was diminished compared to that in siRNA control-treated cells. Interestingly, the replicase activity in the CKB-depleted cells was recovered by the addition of CKB. Thus, our findings suggest that CKB functions as a key regulator of HCV genome replication by controlling energy-dependent viral enzyme activities.

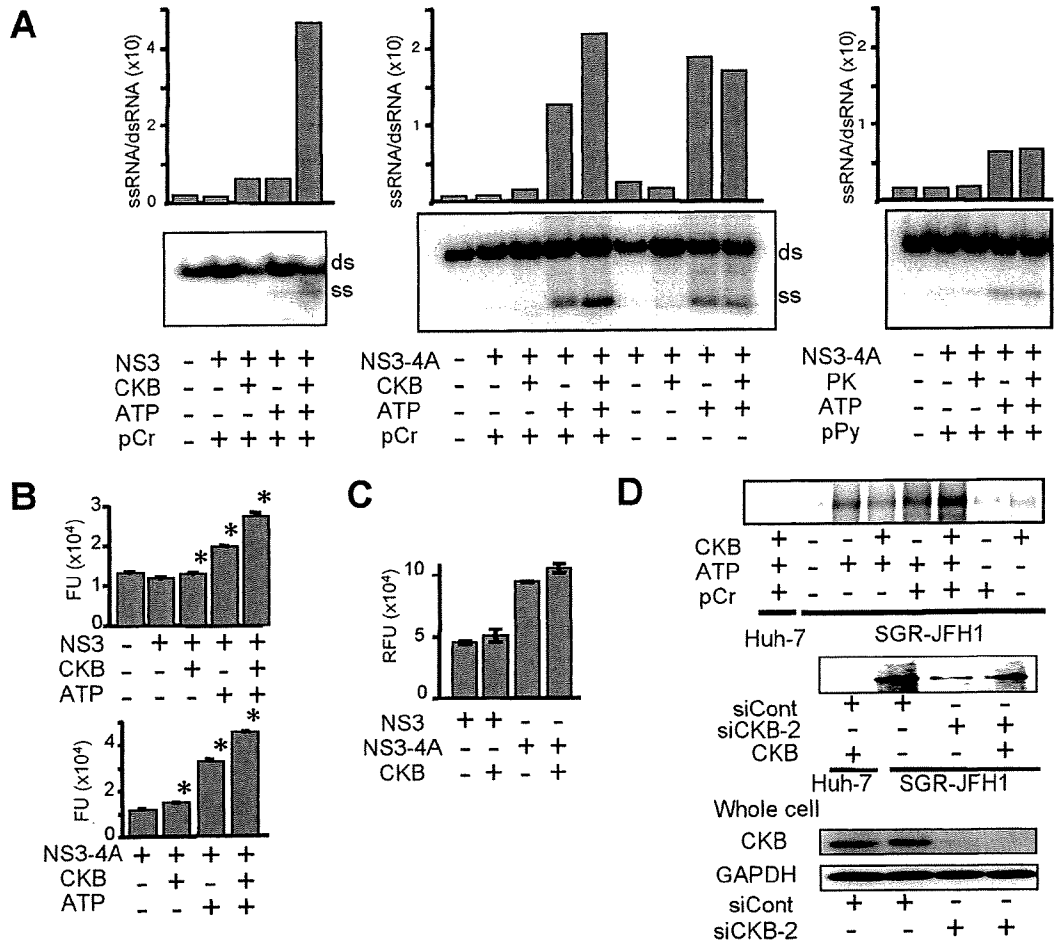

FIG. 5. CKB enhances NS3-4A helicase and HCV replicase activities. (A) In vitro RNA helicase activity of NS3-4A or NS3 was determined by detecting unwound single-strand RNA (ss) derived from the partially dsRNA substrate (ds). Band intensities corresponding to unwound products and those to dsRNA substrates were determined by ImageQuant 5.2 (Molecular Dynamics), and the ssRNA/dsRNA ratios were calculated. The results are representative of three similar experiments. (B) In vitro DNA helicase activity of NS3-4A or NS3 was analyzed by using a commercially available kit. The data represent averages and standard deviations ($n = 3$). *, $P < 0.05$ against the value without supplementation of CKB and ATP. (C) The in vitro HCV protease activity of NS3-4A or NS3 in the presence or absence of CKB was analyzed. Error bars represent standard deviations ($n = 3$). (D) Replicase activity in permeabilized replicon cells. The upper panel shows the activity for synthesis of HCV subgenomic RNA in the digitonin-permeabilized SGR-JFH1 cells with or without supplementation of CKB was measured. The middle panel shows results for SGR-JFH1 or Huh-7 cells that were transfected with siCKB-2 or siCont and permeabilized at 72 h posttransfection. The permeabilized cells with or without supplementation of CKB were subjected to the replicase assay. The lower panel shows the immunoblotting results for whole-cell lysates of siRNA-transfected cells.

DISCUSSION

Viral replication requires energy and macromolecule synthesis, and host cells provide the viruses with metabolic resources necessary for their efficient replication. Thus, it is highly likely that interaction of viruses with host cell metabolic pathways, including energy-generating systems, contributes to the virus growth cycle. In the regulation of HCV genome replication, the functions of the viral NS proteins that comprise the RC might be regulated by association in individual host cell factors. For example, hVAP-A and -B function as cofactors of modulating RC formation via interacting with NS5A and NS5B (13, 18). Cyclophilin B is involved in stimulating viral RNA binding activity via interacting with NS5B (49). FKBP8 (39) and hB-ind1 (45) play an important role in recruiting Hsp90 to RC via interacting with NS5A. However, the association of viral protein(s) with the cellular energy-generating system to directly regulate the activity of the RC has not been well understood.

In the present study, the accumulation of CKB, an ATP-generating enzyme, in the HCV RC-rich membrane fraction of viral replicating cells and its importance in replication of the HCV genome and production of infectious virions have been demonstrated. Enzymatic analyses with semi-intact replicon cells and purified NS3-4A protein revealed that CKB enhances the functional replicase and helicase of HCV. Its enhancing effect was observed in the presence of pCr but not in its absence, suggesting that the catalytic activity of CKB is important for enhancing the replicase and

helicase activities. Moreover, we clearly detected a CKB-NS4A complex using anti-tag antibodies in cotransfection experiments, but the endogenous complex could not be immunoprecipitated from cells expressing only endogenous levels of CKB, probably because of the inefficiency of the available antibodies. Further, a deletion of the NS4A-interacting region within an inactive mutant of CKB (CKB-C283S) resulted in the loss of its dominant-negative effect on HCV replication.

Creatine kinase, an evolutionarily conserved enzyme, is known to be critical for the maintenance and regulation of cellular energy stores in tissues with high and rapidly changing energy demands (48). In mammals, three cytosolic and two mitochondrial isoforms of CK, which share certain conserved regions, are expressed (35). The brain-type CK, CKB, plays a major role in cellular energy metabolism of nonmuscle cells, reversibly catalyzing the ATP-dependent phosphorylation of creatine and, hence, providing an ATP buffering system in subcellular compartments of high and fluctuating energy demand (21, 29). CKB is overexpressed in a wide range of tumor tissues and tumor cell lines, including hepatocellular carcinoma (32), and is used as a prognostic marker of cancer.

Although CK and creatine phosphate have been supplemented to in vitro replicase assays of some RNA viruses (15, 33), understanding of CKB function in the virus life cycle has been limited. One study indicated that the CK substrate analog, Ccr, exhibits antiviral activity against several herpesviruses but not influenza viruses or vesicular stomatitis virus (26). We have demonstrated here that HCV genome replication is downregulated by either treatment with Ccr, siRNA-mediated knockdown of CKB, or the exogenous expression of CKB-C283S. Coimmunoprecipitation experiments revealed that the essential domain within NS4A for the interaction with CKB is the NS4A central domain, aa 21 to 39, which is also responsible for NS3-4A complex formation. However, the NS3-4A interaction was not impaired by overexpression of CKB, and CKB was found to be able to form a complex with NS3-4A (Fig. 3H). Since CKB does not directly interact with NS3 (Fig. 3A), it is likely that NS3-4A-CKB association occurs through two interactions of NS3-4A and NS4A-CKB. We examined whether the formation of the ternary complex affects HCV enzymatic activities, possibly through conformational changes in the viral proteins, and found that CKB has no influence on NS3-4A protease activity (Fig. 5C). With regard to helicase activity, the effect of CKB on RNA unwinding activity by NS3-4A was similar to the effect of NS3 alone in the presence of ATP (Fig. 5A). It is conceivable that interaction with CKB causes no or little global change in the NS3-4A conformation and does not affect the viral helicase and protease activities.

In general, translation initiation in eukaryotes includes an ATP-dependent process such as unwinding the secondary structure in the 5′-untranslated region to permit assembly of 48S ribosomal complexes. It was reported, however, that 48S complex formation on the HCV internal ribosome entry site (IRES) has no requirement for ATP hydrolysis (25). In fact, we found that Huh-7 cells with or without gene silencing of CKB exhibited the same level of HCV IRES activity by transfection with IRES-reporter constructs (data not shown).

Collectively, we conclude that CKB is targeted to the HCV RC through its interaction with NS4A and functions as a positive regulator for the viral replicase by providing ATP. It is likely that the catalytic activity of CKB that associates with the viral RC is important for enhancing the RNA replication. The role of CKB-NS4A interaction in the enhancing effect seems to be limited. Although either knocking down CKB, expression of the dominant-negative mutant of CKB, or Ccr treatment resulted in the reduction of HCV replication (Fig. 2A to C), the total cellular ATP levels were not changed under these conditions (Fig. 2D). This suggests that CKB contributes to enhancing HCV replication through controlling the ATP level in the particular RC compartment. A tight coupling of a fast ATP regeneration and delivery system to the viral RC is advantageous for achieving efficient replication of the viral genome. To our knowledge, the findings presented here provide the first experimental evidence of the involvement of viral protein in recruiting an ATP generating/buffering system to the subcellular compartment for viral genome replication, a site with high-energy turnover. Given that the levels of HCV RNA were not dramatically diminished by the knocking down, dominant-negative mutant or Ccr, CKB may not be absolutely critical for the viral replication. One would argue that energy required for HCV genome replication can be partly complemented from the intracellular ATP pool.

Although there are several isoforms of CK as described above, the most abundant CK species expressed in Huh-7 cells in the present study was CKB, and no other isoenzymes, including mitochondrial CK, were detected by an isoform analysis based on the overlay gel technique (32; data not shown). Thus, the CKB isoenzyme appears to be a key molecule in the energy metabolism of HCV replicating cells. To identify potential HCV RC components, we used a comparative proteome analysis of the DRM fraction in cells harboring HCV subgenomic replicon and the DRM fractions in parental cells and then identified proteins that were more abundant in the fraction of HCV replicating cells. In agreement with similar previously reported approaches using the DRM or lipid raft fraction (30, 53), the functional categories of identified proteins included protein folding or assembly, cell metabolism and biosynthesis, cellular processes, and cytoskeleton organization (Table 1). Interestingly, Mannova et al. found that CKB was upregulated in the fraction of Huh-7 cells carrying the genotype 1b Con1 isolate-derived HCV replicon, as determined using stable isotope labeling by amino acids combined with one-dimensional electrophoresis (30). However, the effect of CKB on regulation of the HCV life cycle was not examined in that study.

In conclusion, CKB interacts with HCV NS4A and is important for efficient replication of the viral genome. Recruitment of CKB to the HCV replication machinery through its interaction with NS4A may have important implications for the maintenance or enhancement of the functional replicase activity in the RC compartment, where high-energy phosphoryl groups are required. A strategy for specific interception of energy supply at the subcellular site of HCV genome replication by disruption of the NS4A-CKB interface may lead to development of a new type of antiviral agent.

ACKNOWLEDGMENTS

We thank Francis V. Chisari (The Scripps Research Institute) for providing Huh-7.5.1 cells; Raffaele De Francesco (Istituto di Ricerche

di Biologia Molecolare, P. Angeletti) for providing purified recombinant NS3 and NS3-4A proteins; Oriental Yeast Co., Ltd., for providing human CKB cDNA; Minoru Fukuda (Laboratory for Electron Microscopy, Kyorin University School of Medicine) for electron microscopy; S. Yoshizaki, T. Shimoji, M. Kaga, M. Sasaki, and T. Date for technical assistance; and T. Mizoguchi for secretarial work.

This study was supported by a grant-in-aid for Scientific Research from the Japan Society for the Promotion of Science, from the Ministry of Health, Labor, and Welfare of Japan and from the Ministry of Education, Culture, Sports, Science, and Technology and by Research on Health Sciences focusing on Drug Innovation from the Japan Health Sciences Foundation, Japan, and by the Program for Promotion of Fundamental Studies in Health Sciences of the National Institute of Biomedical Innovation of Japan.

REFERENCES

1. **Aizaki, H., Y. Aoki, T. Harada, K. Ishii, T. Suzuki, S. Nagamori, G. Toda, Y. Matsuura, and T. Miyamura.** 1998. Full-length complementary DNA of hepatitis C virus genome from an infectious blood sample. Hepatology **27:** 621–627.
2. **Aizaki, H., K. J. Lee, V. M. Sung, H. Ishiko, and M. M. Lai.** 2004. Characterization of the hepatitis C virus RNA replication complex associated with lipid rafts. Virology **324:**450–461.
3. **Aizaki, H., K. Morikawa, M. Fukasawa, H. Hara, Y. Inoue, H. Tani, K. Saito, M. Nishijima, K. Hanada, Y. Matsuura, M. M. Lai, T. Miyamura, T. Wakita, and T. Suzuki.** 2008. Critical role of virion-associated cholesterol and sphingolipid in hepatitis C virus infection. J. Virol. **82:**5715–5724.
4. **Alter, H. J., and L. B. Seeff.** 2000. Recovery, persistence, and sequelae in hepatitis C virus infection: a perspective on long-term outcome. Semin. Liver Dis. **20:**17–35.
5. **Aoyagi, K., C. Ohue, K. Iida, T. Kimura, E. Tanaka, K. Kiyosawa, and S. Yagi.** 1999. Development of a simple and highly sensitive enzyme immunoassay for hepatitis C virus core antigen. J. Clin. Microbiol. **37:**1802–1808.
6. **Appel, N., T. Schaller, F. Penin, and R. Bartenschlager.** 2006. From structure to function: new insights into hepatitis C virus RNA replication. J. Biol. Chem. **281:**9833–9836.
7. **Bartenschlager, R., and V. Lohmann.** 2001. Novel cell culture systems for the hepatitis C virus. Antivir. Res. **52:**1–17.
8. **Brass, V., J. M. Berke, R. Montserret, H. E. Blum, F. Penin, and D. Moradpour.** 2008. Structural determinants for membrane association and dynamic organization of the hepatitis C virus NS3-4A complex. Proc. Natl. Acad. Sci. USA.
9. **Dumont, S., W. Cheng, V. Serebrov, R. K. Beran, I. Tinoco, Jr., A. M. Pyle, and C. Bustamante.** 2006. RNA translocation and unwinding mechanism of HCV NS3 helicase and its coordination by ATP. Nature **439:**105–108.
10. **Failla, C., L. Tomei, and R. De Francesco.** 1994. Both NS3 and NS4A are required for proteolytic processing of hepatitis C virus nonstructural proteins. J. Virol. **68:**3753–3760.
11. **Gallinari, P., D. Brennan, C. Nardi, M. Brunetti, L. Tomei, C. Steinkuhler, and R. De Francesco.** 1998. Multiple enzymatic activities associated with recombinant NS3 protein of hepatitis C virus. J. Virol. **72:**6758–6769.
12. **Gallinari, P., C. Paolini, D. Brennan, C. Nardi, C. Steinkuhler, and R. De Francesco.** 1999. Modulation of hepatitis C virus NS3 protease and helicase activities through the interaction with NS4A. Biochemistry **38:**5620–5632.
13. **Gao, L., H. Aizaki, J. W. He, and M. M. Lai.** 2004. Interactions between viral nonstructural proteins and host protein hVAP-33 mediate the formation of hepatitis C virus RNA replication complex on lipid raft. J. Virol. **78:**3480–3488.
14. **Gosert, R., D. Egger, V. Lohmann, R. Bartenschlager, H. E. Blum, K. Bienz, and D. Moradpour.** 2003. Identification of the hepatitis C virus RNA replication complex in Huh-7 cells harboring subgenomic replicons. J. Virol. **77:**5487–5492.
15. **Green, K. Y., A. Mory, M. H. Fogg, A. Weisberg, G. Belliot, M. Wagner, T. Mitra, E. Ehrenfeld, C. E. Cameron, and S. V. Sosnovtsev.** 2002. Isolation of enzymatically active replication complexes from feline calicivirus-infected cells. J. Virol. **76:**8582–8595.
16. **Guidotti, L. G., and F. V. Chisari.** 2006. Immunobiology and pathogenesis of viral hepatitis. Annu. Rev. Pathol. **1:**23–61.
17. **Guo, J. T., V. V. Bichko, and C. Seeger.** 2001. Effect of alpha interferon on the hepatitis C virus replicon. J. Virol. **75:**8516–8523.
18. **Hamamoto, I., Y. Nishimura, T. Okamoto, H. Aizaki, M. Liu, Y. Mori, T. Abe, T. Suzuki, M. M. Lai, T. Miyamura, K. Moriishi, and Y. Matsuura.** 2005. Human VAP-B is involved in hepatitis C virus replication through interaction with NS5A and NS5B. J. Virol. **79:**13473–13482.
19. **Hoofnagle, J. H.** 2002. Course and outcome of hepatitis C. Hepatology **36:**S21–S29.
20. **Ichimura, T., H. Yamamura, K. Sasamoto, Y. Tominaga, M. Taoka, K. Kakiuchi, T. Shinkawa, N. Takahashi, S. Shimada, and T. Isobe.** 2005. 14-3-3 proteins modulate the expression of epithelial Na+ channels by phosphorylation-dependent interaction with Nedd4-2 ubiquitin ligase. J. Biol. Chem. **280:**13187–13194.
21. **Inoue, K., S. Ueno, and A. Fukuda.** 2004. Interaction of neuron-specific K^+-Cl^- cotransporter, KCC2, with brain-type creatine kinase. FEBS Lett. **564:**131–135.
22. **Inoue, K., J. Yamada, S. Ueno, and A. Fukuda.** 2006. Brain-type creatine kinase activates neuron-specific K^+-Cl^- cotransporter KCC2. J. Neurochem. **96:**598–608.
23. **Kato, T., T. Date, M. Miyamoto, A. Furusaka, K. Tokushige, M. Mizokami, and T. Wakita.** 2003. Efficient replication of the genotype 2a hepatitis C virus subgenomic replicon. Gastroenterology **125:**1808–1817.
24. **Kato, T., A. Furusaka, M. Miyamoto, T. Date, K. Yasui, J. Hiramoto, K. Nagayama, T. Tanaka, and T. Wakita.** 2001. Sequence analysis of hepatitis C virus isolated from a fulminant hepatitis patient. J. Med. Virol. **64:**334–339.
25. **Lancaster, A. M., E. Jan, and P. Sarnow.** 2006. Initiation factor-independent translation mediated by the hepatitis C virus internal ribosome entry site. RNA **12:**894–902.
26. **Lillie, J. W., D. F. Smee, J. H. Huffman, L. J. Hansen, R. W. Sidwell, and R. Kaddurah-Daouk.** 1994. Cyclocreatine (1-carboxymethyl-2-iminoimidazolidine) inhibits the replication of human herpesviruses. Antivir. Res. **23:**203–218.
27. **Lindenbach, B. D., M. J. Evans, A. J. Syder, B. Wolk, T. L. Tellinghuisen, C. C. Liu, T. Maruyama, R. O. Hynes, D. R. Burton, J. A. McKeating, and C. M. Rice.** 2005. Complete replication of hepatitis C virus in cell culture. Science **309:**623–626.
28. **Lindenbach, B. D., B. M. Pragai, R. Montserret, R. K. Beran, A. M. Pyle, F. Penin, and C. M. Rice.** 2007. The C terminus of hepatitis C virus NS4A encodes an electrostatic switch that regulates NS5A hyperphosphorylation and viral replication. J. Virol. **81:**8905–8918.
29. **Mahajan, V. B., K. S. Pai, A. Lau, and D. D. Cunningham.** 2000. Creatine kinase, an ATP-generating enzyme, is required for thrombin receptor signaling to the cytoskeleton. Proc. Natl. Acad. Sci. USA **97:**12062–12067.
30. **Mannova, P., R. Fang, H. Wang, B. Deng, M. W. McIntosh, S. M. Hanash, and L. Beretta.** 2006. Modification of host lipid raft proteome upon hepatitis C virus replication. Mol. Cell Proteomics **5:**2319–2325.
31. **Manos, P., and J. Edmond.** 1992. Immunofluorescent analysis of creatine kinase in cultured astrocytes by conventional and confocal microscopy: a nuclear localization. J. Comp. Neurol. **326:**273–282.
32. **Meffert, G., F. N. Gellerich, R. Margreiter, and M. Wyss.** 2005. Elevated creatine kinase activity in primary hepatocellular carcinoma. BMC Gastroenterol. **5:**9.
33. **Miyanari, Y., M. Hijikata, M. Yamaji, M. Hosaka, H. Takahashi, and K. Shimotohno.** 2003. Hepatitis C virus nonstructural proteins in the probable membranous compartment function in viral genome replication. J. Biol. Chem. **278:**50301–50308.
34. **Moradpour, D., F. Penin, and C. M. Rice.** 2007. Replication of hepatitis C virus. Nat. Rev. Microbiol. **5:**453–463.
35. **Muhlebach, S. M., M. Gross, T. Wirz, T. Wallimann, J. C. Perriard, and M. Wyss.** 1994. Sequence homology and structure predictions of the creatine kinase isoenzymes. Mol. Cell Biochem. **133–134:**245–262.
36. **Murakami, K., K. Ishii, Y. Ishihara, S. Yoshizaki, K. Tanaka, Y. Gotoh, H. Aizaki, M. Kohara, H. Yoshioka, Y. Mori, N. Manabe, I. Shoji, T. Sata, R. Bartenschlager, Y. Matsuura, T. Miyamura, and T. Suzuki.** 2006. Production of infectious hepatitis C virus particles in three-dimensional cultures of the cell line carrying the genome-length dicistronic viral RNA of genotype 1b. Virology **351:**381–392.
37. **Nomura-Takigawa, Y., M. Nagano-Fujii, L. Deng, S. Kitazawa, S. Ishido, K. Sada, and H. Hotta.** 2006. Non-structural protein 4A of Hepatitis C virus accumulates on mitochondria and renders the cells prone to undergoing mitochondria-mediated apoptosis. J. Gen. Virol. **87:**1935–1945.
38. **Ohara-Imaizumi, M., T. Fujiwara, Y. Nakamichi, T. Okamura, Y. Akimoto, J. Kawai, S. Matsushima, H. Kawakami, T. Watanabe, K. Akagawa, and S. Nagamatsu.** 2007. Imaging analysis reveals mechanistic differences between first- and second-phase insulin exocytosis. J. Cell Biol. **177:**695–705.
39. **Okamoto, T., Y. Nishimura, T. Ichimura, K. Suzuki, T. Miyamura, T. Suzuki, K. Moriishi, and Y. Matsuura.** 2006. Hepatitis C virus RNA replication is regulated by FKBP8 and Hsp90. EMBO J. **25:**5015–5025.
40. **Oliver, I. T.** 1955. A spectrophotometric method for the determination of creatine phosphokinase and myokinase. Biochem. J. **61:**116–122.
41. **Shi, S. T., K. J. Lee, H. Aizaki, S. B. Hwang, and M. M. Lai.** 2003. Hepatitis C virus RNA replication occurs on a detergent-resistant membrane that cofractionates with caveolin-2. J. Virol. **77:**4160–4168.
42. **Shirakura, M., K. Murakami, T. Ichimura, R. Suzuki, T. Shimoji, K. Fukuda, K. Abe, S. Sato, M. Fukasawa, Y. Yamakawa, M. Nishijima, K. Moriishi, Y. Matsuura, T. Wakita, T. Suzuki, P. M. Howley, T. Miyamura, and I. Shoji.** 2007. E6AP ubiquitin ligase mediates ubiquitylation and degradation of hepatitis C virus core protein. J. Virol. **81:**1174–1185.
43. **Sunahara, Y., K. Uchida, T. Tanaka, H. Matsukawa, M. Inagaki, and Y. Matuo.** 2001. Production of recombinant human creatine kinase (r-hCK) isozymes by tandem repeat expression of M and B genes and characterization of r-hCK-MB. Clin. Chem. **47:**471–476.

44. **Suzuki, T., K. Ishii, H. Aizaki, and T. Wakita.** 2007. Hepatitis C viral life cycle. Adv. Drug Deliv. Rev. **59:**1200–1212.
45. **Taguwa, S., T. Okamoto, T. Abe, Y. Mori, T. Suzuki, K. Moriishi, and Y. Matsuura.** 2008. Human butyrate-induced transcript 1 interacts with hepatitis C virus NS5A and regulates viral replication. J. Virol. **82:**2631–2641.
46. **Takeuchi, T., A. Katsume, T. Tanaka, A. Abe, K. Inoue, K. Tsukiyama-Kohara, R. Kawaguchi, S. Tanaka, and M. Kohara.** 1999. Real-time detection system for quantification of hepatitis C virus genome. Gastroenterology **116:**636–642.
47. **Wakita, T., T. Pietschmann, T. Kato, T. Date, M. Miyamoto, Z. Zhao, K. Murthy, A. Habermann, H. G. Krausslich, M. Mizokami, R. Bartenschlager, and T. J. Liang.** 2005. Production of infectious hepatitis C virus in tissue culture from a cloned viral genome. Nat. Med. **11:**791–796.
48. **Wallimann, T., M. Wyss, D. Brdiczka, K. Nicolay, and H. M. Eppenberger.** 1992. Intracellular compartmentation, structure and function of creatine kinase isoenzymes in tissues with high and fluctuating energy demands: the 'phosphocreatine circuit' for cellular energy homeostasis. Biochem. J. **281**(Pt. 1):21–40.
49. **Watashi, K., N. Ishii, M. Hijikata, D. Inoue, T. Murata, Y. Miyanari, and K. Shimotohno.** 2005. Cyclophilin B is a functional regulator of hepatitis C virus RNA polymerase. Mol. Cell **19:**111–122.
50. **Wolk, B., D. Sansonno, H. G. Krausslich, F. Dammacco, C. M. Rice, H. E. Blum, and D. Moradpour.** 2000. Subcellular localization, stability, and trans-cleavage competence of the hepatitis C virus NS3-NS4A complex expressed in tetracycline-regulated cell lines. J. Virol. **74:**2293–2304.
51. **Wyss, M., and R. Kaddurah-Daouk.** 2000. Creatine and creatinine metabolism. Physiol. Rev. **80:**1107–1213.
52. **Yi, M., R. A. Villanueva, D. L. Thomas, T. Wakita, and S. M. Lemon.** 2006. Production of infectious genotype 1a hepatitis C virus (Hutchinson strain) in cultured human hepatoma cells. Proc. Natl. Acad. Sci. USA **103:**2310–2315.
53. **Yi, Z., C. Fang, T. Pan, J. Wang, P. Yang, and Z. Yuan.** 2006. Subproteomic study of hepatitis C virus replicon reveals Ras-GTPase-activating protein binding protein 1 as potential HCV RC component. Biochem. Biophys. Res. Commun. **350:**174–178.
54. **Zhong, J., P. Gastaminza, G. Cheng, S. Kapadia, T. Kato, D. R. Burton, S. F. Wieland, S. L. Uprichard, T. Wakita, and F. V. Chisari.** 2005. Robust hepatitis C virus infection in vitro. Proc. Natl. Acad. Sci. USA **102:**9294–9299.

JOURNAL OF VIROLOGY, Mar. 2009, p. 2389–2392 Vol. 83, No. 5
0022-538X/09/$08.00+0 doi:10.1128/JVI.01690-08

Proteasomal Turnover of Hepatitis C Virus Core Protein Is Regulated by Two Distinct Mechanisms: a Ubiquitin-Dependent Mechanism and a Ubiquitin-Independent but PA28γ-Dependent Mechanism▽

Ryosuke Suzuki,[1] Kohji Moriishi,[2] Kouichirou Fukuda,[1] Masayuki Shirakura,[1] Koji Ishii,[1] Ikuo Shoji,[3] Takaji Wakita,[1] Tatsuo Miyamura,[1] Yoshiharu Matsuura,[2] and Tetsuro Suzuki[1]*

Department of Virology II, National Institute of Infectious Diseases, Tokyo 162-8640,[1] Department of Molecular Virology, Research Institute for Microbial Diseases, Osaka University, Osaka 565-0871,[2] and Division of Microbiology, Kobe University Graduate School of Medicine, Hyogo 650-0017,[3] Japan

Received 8 August 2008/Accepted 5 December 2008

We have previously reported on the ubiquitylation and degradation of hepatitis C virus core protein. Here we demonstrate that proteasomal degradation of the core protein is mediated by two distinct mechanisms. One leads to polyubiquitylation, in which lysine residues in the N-terminal region are preferential ubiquitylation sites. The other is independent of the presence of ubiquitin. Gain- and loss-of-function analyses using lysineless mutants substantiate the hypothesis that the proteasome activator PA28γ, a binding partner of the core, is involved in the ubiquitin-independent degradation of the core protein. Our results suggest that turnover of this multifunctional viral protein can be tightly controlled via dual ubiquitin-dependent and -independent proteasomal pathways.

Hepatitis C virus (HCV) core protein, whose amino acid sequence is highly conserved among different HCV strains, not only is involved in the formation of the HCV virion but also has a number of regulatory functions, including modulation of signaling pathways, cellular and viral gene expression, cell transformation, apoptosis, and lipid metabolism (reviewed in references 9 and 15). We have previously reported that the E6AP E3 ubiquitin (Ub) ligase binds to the core protein and plays an important role in polyubiquitylation and proteasomal degradation of the core protein (22). Another study from our group identified the proteasome activator PA28γ/REG-γ as an HCV core-binding partner, demonstrating degradation of the core protein via a PA28γ-dependent pathway (16, 17). In this work, we further investigated the molecular mechanisms underlying proteasomal degradation of the core protein and found that in addition to regulation by the Ub-mediated pathway, the turnover of the core protein is also regulated by PA28γ in a Ub-independent manner.

Although ubiquitylation of substrates generally requires at least one Lys residue to serve as a Ub acceptor site (5), there is no consensus as to the specificity of the Lys targeted by Ub (4, 8). To determine the sites of Ub conjugation in the core protein, we used site-directed mutagenesis to replace individual Lys residues or clusters of Lys residues with Arg residues in the N-terminal 152 amino acids (aa) of the core (C152), within which is contained all seven Lys residues (Fig. 1A). Plasmids expressing a variety of mutated core proteins were generated by PCR and inserted into the pCAGGS (18). Each core-expressing construct was transfected into human embryonic kidney 293T cells along with the pMT107 (25) encoding a Ub moiety tagged with six His residues (His_6). Transfected cells were treated with the proteasome inhibitor MG132 for 14 h to maximize the level of Ub-conjugated core intermediates by blocking the proteasome pathway and were harvested 48 h posttransfection. His_6-tagged proteins were purified from the extracts by Ni^{2+}-chelation chromatography. Eluted protein and whole lysates of transfected cells before purification were analyzed by Western blotting using anticore antibodies (Fig. 1B). Mutations replacing one or two Lys residues with Arg in the core protein did not affect the efficiency of ubiquitylation: detection of multiple Ub-conjugated core intermediates was observed in the mutant core proteins comparable to the results seen with the wild-type core protein as previously reported (23). In contrast, a substitution of four N-terminal Lys residues (C152K6-23R) caused a significant reduction in ubiquitylation (Fig. 1B, lane 9). Multiple Ub-conjugated core intermediates were not detected in the Lys-less mutant (C152KR), in which all seven Lys residues were replaced with Arg (Fig. 1B, lane 11). These results suggest that there is not a particular Lys residue in the core protein to act as the Ub acceptor but that more than one Lys located in its N-terminal region can serve as the preferential ubiquitylation site. In rare cases, Ub is known to be conjugated to the N terminus of proteins; however, these results indicate that this does not occur within the core protein.

To investigate how polyubiquitylation correlates with proteasome degradation of the core protein, we performed kinetic analysis of the wild-type and mutated core proteins by use of the Ub protein reference (UPR) technique, which can compensate for data scatter of sample-to-sample variations such as levels of expression (10, 24). Fusion proteins expressed from UPR-based constructs (Fig. 2A) were cotranslationally cleaved by deubiquitylating enzymes, thereby generating equimolar quantities of the core proteins and the reference protein, dihydrofolate reductase-hemagglutinin (DHFR-HA) tag-modified Ub, in which the Lys at aa 48 was replaced by Arg to prevent its polyubiquitylation (Ub^{R48}). After 24 h of transfec-

* Corresponding author. Mailing address: Department of Virology II, National Institute of Infectious Diseases, 1-23-1 Toyama, Shinjuku-ku, Tokyo 162-8640, Japan. Phone: 81-3-5285-1111. Fax: 81-3-5285-1161. E-mail: tesuzuki@nih.go.jp.

▽ Published ahead of print on 17 December 2008.

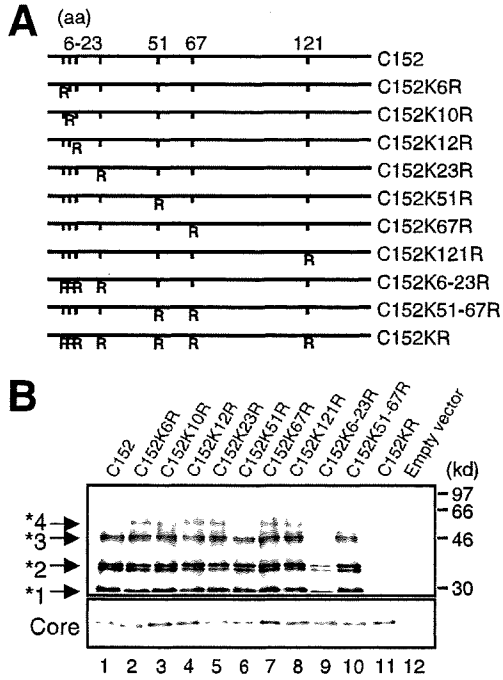

FIG. 1. In vivo ubiquitylation of HCV core protein. (A) The HCV core protein (N-terminal 152 aa) is represented on the top. The positions of the amino acid residues of the core protein are indicated above the bold lines. The positions of the seven Lys residues in the core are marked by vertical ticks. Substitution of Lys with Arg (R) is schematically depicted. (B) Detection of ubiquitylated forms of the core proteins. The transfected cells with core expression plasmids and pMT107 were treated with the proteasome inhibitor MG132 and harvested 48 h after transfection. His_6-tagged proteins were purified and subsequently analyzed by Western blot analysis using anticore antibody (upper panel). Core proteins conjugated to a number of His_6-Ub are denoted with asterisks. Whole lysates of transfected cells before purification were also analyzed (lower panel). Lanes 1 to 11, C152 to C152KR, as indicated for panel A. Lane 12; empty vector.

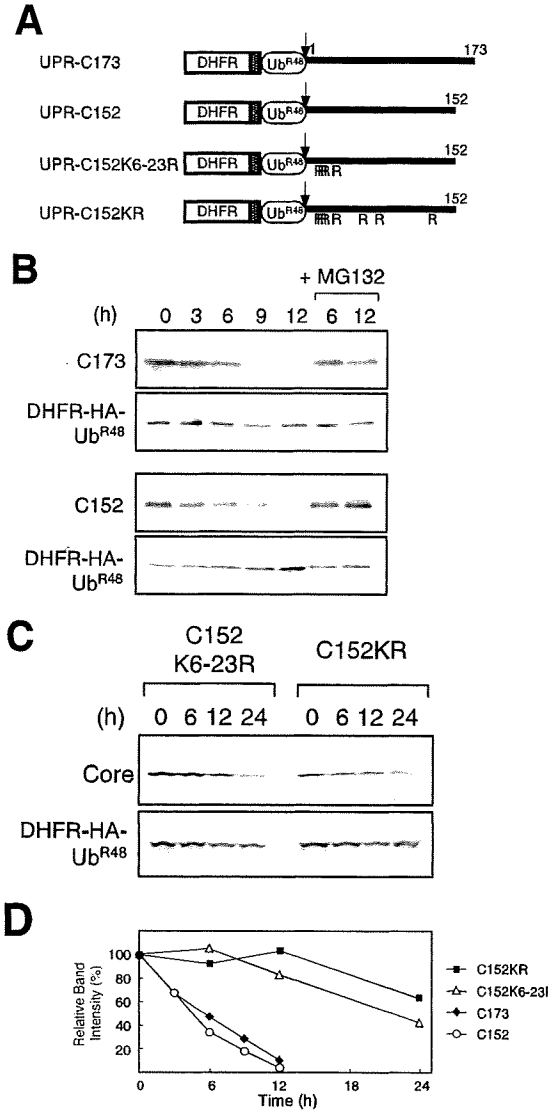

FIG. 2. Kinetic analysis of degradation of HCV core proteins. (A) The fusion constructs used in the UPR technique. Open boxes indicate the DHFR sequence, which is extended at the C terminus by a sequence containing the HA epitope (hatched boxes). Ub^{R48} moieties bearing the Lys-Arg substitution at aa 48 are represented by open ellipses. Bold lines indicate the regions of the core protein. The amino acid positions of the core protein are indicated above the bold lines. The arrows indicate the sites of in vivo cleavage by deubiquitylating enzymes. (B and C) Turnover of the core proteins. After a 24-h transfection with each UPR construct, cells were treated with 50 μg of cycloheximide/ml in the presence or absence of 10 μM MG132 for the different time periods indicated. Cells were lysed at the different time points indicated, followed by evaluation via sodium dodecyl sulfate-polyacrylamide gel electrophoresis and Western blot analysis using antibodies against the core protein and HA. (D) Quantitation of the data shown in panels B and C. At each time point, the ratio of band intensity of the core protein relative to the reference DHFR-HA-Ub^{R48} was determined by densitometry and is plotted as a percentage of the ratio at time zero.

tion with UPR constructs, cells were treated with cycloheximide and the amounts of core proteins and DHFR-HA-Ub^{R48} at the indicated time points were determined by Western blot analysis using anticore and anti-HA antibodies. The mature form of the core protein, aa 1 to 173 (C173) (13, 20), and C152 were degraded with first-order kinetics (Fig. 2B and D). MG132 completely blocked the degradation of C173 and C152 (Fig. 2B), and C152K6-23R and C152KR were markedly stabilized (Fig. 2C). The half-lives of C173 and C152 were calculated to be 5 to 6 h, whereas those of C152K6-23R and C152KR were calculated to be 22 to 24 h (Fig. 2D), confirming that the Ub plays an important role in regulating degradation of the core protein. Nevertheless, these results also suggest possible involvement of the Ub-independent pathway in the turnover of the core protein, as C152KR is more destabilized than the reference protein (Fig. 2C and 2D).

We have shown that PA28γ specifically binds to the core protein and is involved in its degradation (16, 17). Recent studies demonstrated that PA28γ is responsible for Ub-independent degradation of the steroid receptor coactivator SRC-3 and cell cycle inhibitors such as p21 (3, 11, 12). Thus, we next investigated the possibility of PA28γ involvement in the degradation of either C152KR or C152. Since C152KR carries two amino acid substitutions in the PA28γ-binding region (aa 44 to 71) (17), we tested the influence of the mutations of C152KR on the interaction with PA28γ by use of a coimmunoprecipi-

tation assay. When Flag-tagged PA28γ (F-PA28γ) was expressed in cells along with C152 or C152KR, F-PA28γ precipitated along with both C152 and C152KR, indicating that PA28γ interacts with both core proteins (Fig. 3A). Figure 3B reveals the effect of exogenous expression of F-PA28γ on the steady-state levels of C152 and C152KR. Consistent with previous data (17), the expression level of C152 was decreased to a nearly undetectable level in the presence of PA28γ (Fig. 3B, lanes 1 and 3). Interestingly, exogenous expression of PA28γ led to a marked reduction in the amount of C152KR expressed (Fig. 3B, lanes 5 and 7). Treatment with MG132 increased the steady-state level of the C152KR in the presence of F-PA28γ as well as the level of C152 (Fig. 3B, lanes 4 and 8).

We further investigated whether PA28γ affects the turnover of Lys-less core protein through time course experiments. C152KR was rapidly destabilized and almost completely degraded in a 3-h chase experiment using cells overexpressing F-PA28γ (Fig. 3C, left panels). A similar result was obtained using an analogous Lys-less mutant of the full-length core protein C191KR (Fig. 3C, right panels), thus demonstrating that the Lys-less core protein undergoes proteasomal degradation in a PA28γ-dependent manner. These results suggest that PA28γ may play a role in accelerating the turnover of the HCV core protein that is independent of ubiquitylation.

Finally, we examined gain- and loss-of-function of PA28γ with respect to degradation of full-length wild-type (C191) and mutated (C191KR) core proteins in human hepatoma Huh-7 cells. As expected, exogenous expression of PA28γ or E6AP caused a decrease in the C191 steady-state levels (Fig. 4A). In contrast, the C191KR level was decreased with expression of PA28γ but not of E6AP. We further used RNA interference to inhibit expression of PA28γ or E6AP. An increase in the abundance of C191KR was observed with PA28γ small interfering RNA (siRNA) but not with E6AP siRNA (Fig. 4B). An increase in the C191 level caused by the activity of siRNA against PA28γ or E6AP was confirmed as well.

Taking these results together, we conclude that turnover of the core protein is regulated by both Ub-dependent and Ub-independent pathways and that PA28γ is possibly involved in Ub-independent proteasomal degradation of the core protein. PA28 is known to specifically bind and activate the 20S proteasome (19). Thus, PA28γ may function by facilitating the delivery of the core protein to the proteasome in a Ub-independent manner.

Accumulating evidence suggests the existence of proteasome-dependent but Ub-independent pathways for protein degradation, and several important molecules, such as p53, p73, Rb, SRC-3, and the hepatitis B virus X protein, have two distinct degradation pathways that function in a Ub-dependent and Ub-independent manner (1, 2, 6, 7, 14, 21, 27). Recently, critical roles for PA28γ in the Ub-independent pathway have been demonstrated; SRC-3 and p21 can be recognized by the 20S proteasome independently of ubiquitylation through their interaction with PA28γ (3, 11, 12). It has also been reported that phosphorylation-dependent ubiquitylation mediated by GSK3 and SCF is important for SRC-3 turnover (26). Nevertheless, the precise mechanisms underlying turnover of most of the proteasome substrates that are regulated in both Ub-dependent and Ub-independent manners are not well understood. To our knowledge, the HCV core protein is the first

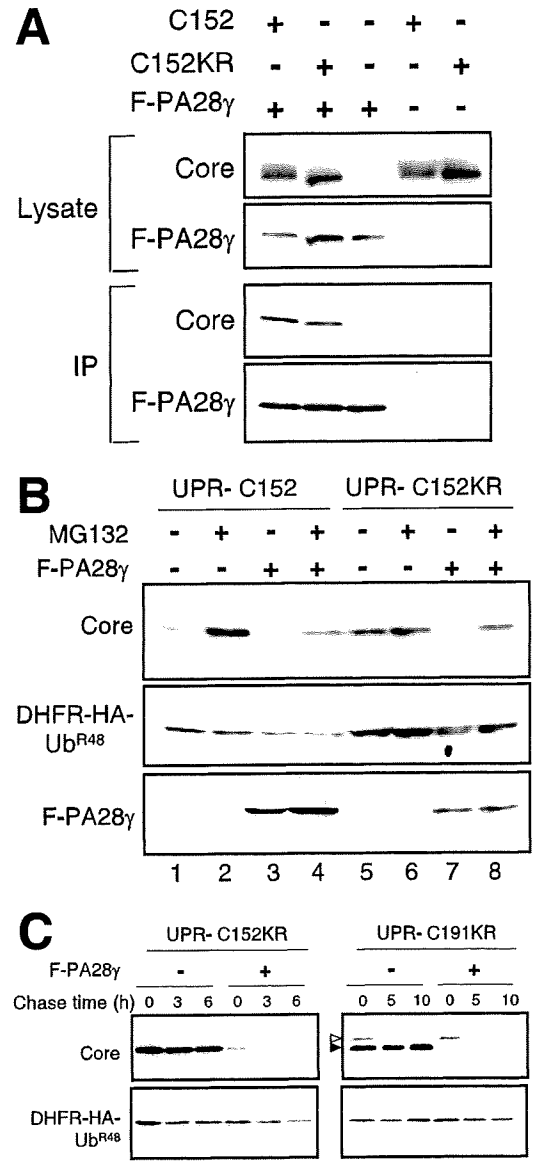

FIG. 3. PA28γ-dependent degradation of the core protein. (A) Interaction of the core protein with PA28γ. Cells were cotransfected with the wild-type (C152) or Lys-less (C152KR) core expression plasmid in the presence of a Flag-PA28γ (F-PA28γ) expression plasmid or an empty vector. The transfected cells were treated with MG132. After 48 h, the cell lysates were immunoprecipitated with anti-Flag antibody and visualized by Western blotting with anticore antibodies. Western blot analysis of whole cell lysates was also performed. (B) Degradation of the wild-type and Lys-less core proteins via the PA28γ-dependent pathway. Cells were transfected with the UPR construct with or without F-PA28γ. In some cases, cells were treated with 10 μM MG132 for 14 h before harvesting. Western blot analysis was performed using anticore, anti-HA, and anti-Flag antibodies. (C) After 24 h of transfection with UPR-C152KR and UPR-C191KR with or without F-PA28γ (an empty vector), cells were treated with 50 μg of cycloheximide/ml for different time periods as indicated (chase time). Western blot analysis was performed using anticore and anti-HA antibodies. The precursor core protein and the core that was processed, presumably by signal peptide peptidase, are denoted by open and closed triangles, respectively.

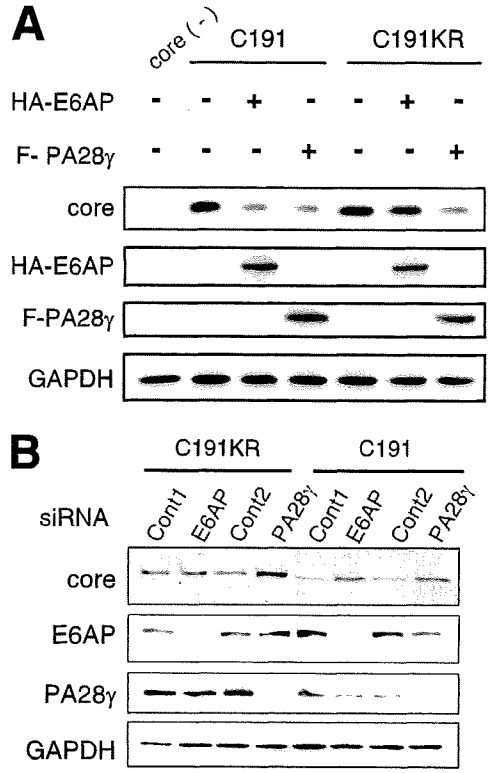

FIG. 4. Ub-dependent and Ub-independent degradation of the full-length core protein in hepatic cells. (A) Huh-7 cells were cotransfected with plasmids for the full-length core protein (C191) or its Lys-less mutant (C191KR) in the presence of F-PA28γ or HA-tagged-E6AP expression plasmid (HA-E6AP). After 48 h, cells were lysed and Western blot analysis was performed using anticore, anti-HA, anti-Flag, or anti-GAPDH. (B) Huh-7 cells were cotransfected with core expression plasmids along with siRNA against PA28γ or E6AP or with negative control siRNA. Cells were harvested 72 h after transfection and subjected to Western blot analysis.

viral protein studied that has led to identification of key cellular factors responsible for proteasomal degradation via dual distinct mechanisms. Although the question remains whether there is a physiological significance of the Ub-dependent and Ub-independent degradation of the core protein, it is reasonable to consider that tight control over cellular levels of the core protein, which is multifunctional and essential for viral replication, maturation, and pathogenesis, may play an important role in representing the potential for its functional activity.

This work was supported by a grant-in-aid for Scientific Research from the Japan Society for the Promotion of Science, from the Ministry of Health, Labor and Welfare of Japan, and from the Ministry of Education, Culture, Sports, Science and Technology, by Research on Health Sciences focusing on Drug Innovation from the Japan Health Sciences Foundation, Japan, and by the Program for Promotion of Fundamental Studies in Health Sciences of the National Institute of Biomedical Innovation of Japan.

REFERENCES

1. **Asher, G., J. Lotem, L. Sachs, C. Kahana, and Y. Shaul.** 2002. Mdm-2 and ubiquitin-independent p53 proteasomal degradation regulated by NQO1. Proc. Natl. Acad. Sci. USA **99:**13125–13130.
2. **Asher, G., P. Tsvetkov, C. Kahana, and Y. Shaul.** 2005. A mechanism of ubiquitin-independent proteasomal degradation of the tumor suppressors p53 and p73. Genes Dev. **19:**316–321.
3. **Chen, X., L. F. Barton, Y. Chi, B. E. Clurman, and J. M. Roberts.** 2007. Ubiquitin-independent degradation of cell-cycle inhibitors by the REGγ proteasome. Mol. Cell **26:**843–852.
4. **Ciechanover, A.** 1998. The ubiquitin-proteasome pathway: on protein death and cell life. EMBO J. **17:**7151–7160.
5. **Hershko, A., A. Ciechanover, and A. Varshavsky.** 2000. The ubiquitin system. Nat. Med. **6:**1073–1081.
6. **Jariel-Encontre, I., M. Pariat, F. Martin, S. Carillo, C. Salvat, and M. Piechaczyk.** 1995. Ubiquitinylation is not an absolute requirement for degradation of c-Jun protein by the 26 S proteasome. J. Biol. Chem. **270:**11623–11627.
7. **Jin, Y., H. Lee, S. X. Zeng, M. S. Dai, and H. Lu.** 2003. MDM2 promotes p21waf1/cip1 proteasomal turnover independently of ubiquitylation. EMBO J. **22:**6365–6377.
8. **Ju, D., and Y. Xie.** 2006. Identification of the preferential ubiquitination site and ubiquitin-dependent degradation signal of Rpn4. J. Biol. Chem. **281:**10657–10662.
9. **Lai, M. M. C., and C. F. Ware.** 1999. Hepatitis C virus core protein: possible roles in viral pathogenesis. Springer, Berlin, Germany.
10. **Lévy, F., N. Johnsson, T. Rumenapf, and A. Varshavsky.** 1996. Using ubiquitin to follow the metabolic fate of a protein. Proc. Natl. Acad. Sci. USA **93:**4907–4912.
11. **Li, X., L. Amazit, W. Long, D. M. Lonard, J. J. Monaco, and B. W. O'Malley.** 2007. Ubiquitin- and ATP-independent proteolytic turnover of p21 by the REGγ-proteasome pathway. Mol. Cell **26:**831–842.
12. **Li, X., D. M. Lonard, S. Y. Jung, A. Malovannaya, Q. Feng, J. Qin, S. Y. Tsai, M. J. Tsai, and B. W. O'Malley.** 2006. The SRC-3/AIB1 coactivator is degraded in a ubiquitin- and ATP-independent manner by the REGγ proteasome. Cell **124:**381–392.
13. **Liu, Q., C. Tackney, R. A. Bhat, A. M. Prince, and P. Zhang.** 1997. Regulated processing of hepatitis C virus core protein is linked to subcellular localization. J. Virol. **71:**657–662.
14. **Lonard, D. M., Z. Nawaz, C. L. Smith, and B. W. O'Malley.** 2000. The 26S proteasome is required for estrogen receptor-α and coactivator turnover and for efficient estrogen receptor-α transactivation. Mol. Cell **5:**939–948.
15. **Moradpour, D., F. Penin, and C. M. Rice.** 2007. Replication of hepatitis C virus. Nat. Rev. Microbiol. **5:**453–463.
16. **Moriishi, K., R. Mochizuki, K. Moriya, H. Miyamoto, Y. Mori, T. Abe, S. Murata, K. Tanaka, T. Miyamura, T. Suzuki, K. Koike, and Y. Matsuura.** 2007. Critical role of PA28γ in hepatitis C virus-associated steatogenesis and hepatocarcinogenesis. Proc. Natl. Acad. Sci. USA **104:**1661–1666.
17. **Moriishi, K., T. Okabayashi, K. Nakai, K. Moriya, K. Koike, S. Murata, T. Chiba, K. Tanaka, R. Suzuki, T. Suzuki, T. Miyamura, and Y. Matsuura.** 2003. Proteasome activator PA28γ-dependent nuclear retention and degradation of hepatitis C virus core protein. J. Virol. **77:**10237–10249.
18. **Niwa, H., K. Yamamura, and J. Miyazaki.** 1991. Efficient selection for high-expression transfectants with a novel eukaryotic vector. Gene **108:**193–199.
19. **Realini, C., C. C. Jensen, Z. Zhang, S. C. Johnston, J. R. Knowlton, C. P. Hill, and M. Rechsteiner.** 1997. Characterization of recombinant REGα, REGβ, and REGγ proteasome activators. J. Biol. Chem. **272:**25483–25492.
20. **Santolini, E., G. Migliaccio, and N. La Monica.** 1994. Biosynthesis and biochemical properties of the hepatitis C virus core protein. J. Virol. **68:**3631–3641.
21. **Sheaff, R. J., J. D. Singer, J. Swanger, M. Smitherman, J. M. Roberts, and B. E. Clurman.** 2000. Proteasomal turnover of p21Cip1 does not require p21Cip1 ubiquitination. Mol. Cell **5:**403–410.
22. **Shirakura, M., K. Murakami, T. Ichimura, R. Suzuki, T. Shimoji, K. Fukuda, K. Abe, S. Sato, M. Fukasawa, Y. Yamakawa, M. Nishijima, K. Moriishi, Y. Matsuura, T. Wakita, T. Suzuki, P. M. Howley, T. Miyamura, and I. Shoji.** 2007. E6AP ubiquitin ligase mediates ubiquitylation and degradation of hepatitis C virus core protein. J. Virol. **81:**1174–1185.
23. **Suzuki, R., K. Tamura, J. Li, K. Ishii, Y. Matsuura, T. Miyamura, and T. Suzuki.** 2001. Ubiquitin-mediated degradation of hepatitis C virus core protein is regulated by processing at its carboxyl terminus. Virology **280:**301–309.
24. **Suzuki, T., and A. Varshavsky.** 1999. Degradation signals in the lysine-asparagine sequence space. EMBO J. **18:**6017–6026.
25. **Treier, M., L. M. Staszewski, and D. Bohmann.** 1994. Ubiquitin-dependent c-Jun degradation in vivo is mediated by the δ domain. Cell **78:**787–798.
26. **Wu, R. C., Q. Feng, D. M. Lonard, and B. W. O'Malley.** 2007. SRC-3 coactivator functional lifetime is regulated by a phospho-dependent ubiquitin time clock. Cell **129:**1125–1140.
27. **Zhang, Z., and R. Zhang.** 2008. Proteasome activator PA28γ regulates p53 by enhancing its MDM2-mediated degradation. EMBO J. **27:**852–864.

THE JOURNAL OF BIOLOGICAL CHEMISTRY VOL. 284, NO. 8, pp. 5067–5076, February 20, 2009

Rho-kinase Contributes to Sustained RhoA Activation through Phosphorylation of p190A RhoGAP*[S]

Received for publication, September 4, 2008, and in revised form, December 4, 2008 Published, JBC Papers in Press, December 22, 2008, DOI 10.1074/jbc.M806853200

Kazutaka Mori[‡§1], Mutsuki Amano[‡1], Mikito Takefuji[‡§], Katsuhiro Kato[‡§], Yasuhiro Morita[‡§], Tomoki Nishioka[‡¶], Yoshiharu Matsuura[‖], Toyoaki Murohara[§], and Kozo Kaibuchi[‡2]

From the Departments of [‡] Cell Pharmacology, and [§] Cardiology, Graduate School of Medicine, Nagoya University, 65 Tsurumai, Showa-ku, Nagoya 466-8550, the [¶]Department of Forensic Medicine and Human Genetics, Kurume University School of Medicine, Kurume 830-0011, and the [‖]Department of Molecular Virology, Research Institute for Microbial Diseases, Osaka University, Osaka 565-0871, Japan

RhoA is transiently activated by specific extracellular signals such as endothelin-1 (ET-1) in vascular smooth muscle cells. RhoGAP negatively regulates RhoA activity: thus, RhoA becomes the GDP-bound inactive form afterward. Sustained activation of RhoA is induced with high doses of the extracellular signals and is implicated in certain diseases such as vasospasms. However, it remains largely unknown how prolonged activation of RhoA is induced. Here we show that Rho-kinase, an effector of RhoA, phosphorylated p190A RhoGAP at Ser^{1150} and attenuated p190A RhoGAP activity in COS7 cells. Binding of Rnd to p190A RhoGAP is thought to enhance its activation. Phosphorylation of p190A RhoGAP by Rho-kinase impaired Rnd binding. Stimulation of vascular smooth muscle cells with a high dose of ET-1 provoked sustained RhoA activation and p190A RhoGAP phosphorylation, both of which were prohibited by a Rho-kinase inhibitor. The phosphomimic mutation of p190A RhoGAP weakened Rnd binding and RhoGAP activities. Taken together, these results suggest that ET-1 induces Rho-kinase activation and subsequent phosphorylation of p190A RhoGAP, leading to prolonged RhoA activation.

RhoA small GTPase is the molecular switch for various extracellular signals and is implicated in a variety of biological functions, including cell contraction, cell migration, cell adhesion, cell cycle progression, and gene expression (1, 2). RhoA regulates these functions through its specific effectors such as Rho-kinase/ROCK/ROK and mDia (2). We previously found that Rho-kinase phosphorylates myosin phosphatase target protein 1 (MYPT1)[3] of myosin phosphatase and thereby inactivates its phosphatase activity, resulting in an increase in the phosphorylation of myosin light chain followed by smooth muscle contraction (3–5). Rho-kinase increases the agonist-induced Ca^{2+} sensitivity and contributes to sustained contraction of smooth muscle (6).

RhoA cycles between the GTP-bound active and GDP-bound inactive conformations. This cycle is under the direct control of three groups of regulatory proteins: the guanine nucleotide exchange factors (GEFs), which catalyze the exchange of GDP for GTP to activate RhoA; GTPase-activating proteins (GAPs), which enhance the intrinsic GTPase activity of RhoA to promote hydrolysis of GTP to GDP to inactivate RhoA; and the guanine nucleotide dissociation inhibitors, which sequester the GDP-bound RhoA and may also regulate its intracellular localization (1, 2).

The typical RhoGEFs contain a catalytic Dbl homology domain and an adjacent pleckstrin homology domain. This Dbl homology-associated pleckstrin homology domain interacts with phospholipids, which may localize GEFs to the plasma membrane and activate GEF activity (7, 8). RhoA activation is often mediated by G protein-coupled receptors. Three RhoGEFs, which contain the regulator of G protein-signaling domains, including leukemia-associated RhoGEF, PDZ-RhoGEF, and p115RhoGEF, directly link between $G\alpha_{12}/G\alpha_{13}$ and RhoA (9–11). $G\alpha_{12}$ and $G\alpha_{13}$ specifically interact with the regulator of G protein-signaling domains of these RhoGEFs and positively regulate their GEF activity (12). The typical RhoGAPs have a catalytic domain and various domains for protein-protein interaction. Recent studies suggest that RhoGAPs are regulated by various mechanisms, including protein-protein interaction, phospholipid interaction, phosphorylation, subcellular translocation, and proteolytic degradation (13, 14). However, the precise mechanisms that regulate RhoGAP activity remain elusive in many cases.

When the smooth muscle cells are stimulated with agonists such as ET-1, RhoA is transiently activated presumably through RhoA-specific GEFs such as leukemia-associated RhoGEF and inactivated later (11, 15). The RhoA-specific GAP appears to be responsible for RhoA inactivation under physiological conditions (16). Sustained RhoA/Rho-kinase activation occurs with

* This work was supported by grants-in-aid for creative science research and a grant-in-aid for scientific research (S: 20227006; C: 20590308), by the Global Centers of Excellence Program from the Ministry of Education, Culture, Sports, Science, and Technology of Japan, and by the Program for Promotion of Fundamental Studies in Health Sciences of the National Institute of Biomedical Innovation (Grant 02-3). The costs of publication of this article were defrayed in part by the payment of page charges. This article must therefore be hereby marked "*advertisement*" in accordance with 18 U.S.C. Section 1734 solely to indicate this fact.

[S] The on-line version of this article (available at http://www.jbc.org) contains supplemental Figs. S1–S5.

[1] Both authors contributed equally to this work.

[2] To whom correspondence should be addressed. Tel.: 81-52-744-2074; Fax: 81-52-744-2083; E-mail: kaibuchi@med.nagoya-u.ac.jp.

[3] The abbreviations used are: MYPT1, myosin phosphatase target protein-1; ET-1, endothelin-1; GEF, guanine nucleotide exchange factor; GAP, GTPase-activating protein; FL, full length; RBD, Rho-binding domain; WT, wild-type; GFP, green fluorescent protein; GST, glutathione *S*-transferase; aa, amino acid(s); HA, hemagglutinin; Ab, antibody.

high doses of ET-1 (17). Prolonged activation of RhoA/Rho-kinase is implicated in the pathogenesis of certain vascular diseases, including subarachnoid hemorrhage-induced cerebral vasospasm, coronary vasospasm, essential hypertension, and pulmonary hypertension (18, 19). For example, RhoA activity is higher in aortic smooth muscle cells derived from the stroke-prone spontaneously hypertensive rat than from the wild-type rat, although the expression levels of RhoA are not different between mutant and wild-type rats (20). Rho-kinase activity is up-regulated, and phosphorylation levels of MYPT1 are increased in the coronary spastic lesion in a porcine swine model (21). Subarachnoid hemorrhage induces sustained Rho-kinase activation in the canine basilar artery and subsequent cerebral vasospasm (22). Chronic hypoxia-induced pulmonary hypertension in rats is associated with an increase of RhoA activity in pulmonary artery (23). However, it remains largely unknown how prolonged activation of RhoA is induced.

In light of these observations, we hypothesized that highly activated RhoA/Rho-kinase can inhibit Rho-specific GAP and lead to sustained RhoA activation. Here we show that Rho-kinase phosphorylated p190A RhoGAP, the best characterized RhoA-specific GAP, at Ser^{1150} *in vitro* and *in vivo*. Phosphorylation of p190A RhoGAP by Rho-kinase appeared to attenuate its GAP activity.

EXPERIMENTAL PROCEDURES

Materials and Chemicals—The cDNA-encoding human p190A RhoGAP (KIAA1722, p190A) was obtained from the Kazusa DNA Research Institute (Chiba, Japan). Monoclonal anti-GFP antibody was purchased from Roche Diagnostics (Mannheim, Germany). Polyclonal anti-GFP antibody was from MBL (Nagoya, Japan). Monoclonal anti-p190A RhoGAP antibodies were from BD Biosciences Pharmingen (San Diego, CA) and Upstate Biotechnology (Lake Placid, NY). Monoclonal anti-RhoA antibody was from Santa Cruz Biotechnology, Inc. (Santa Cruz, CA). Monoclonal anti-HA antibody (12CA5) was from Boehringer (Ingelheim, Germany). Polyclonal anti-MYPT1-pT853 antibody was from Upstate Biotechnology. Polyclonal anti-total MYPT1 antibody was generated as previously described (24). A rabbit polyclonal antibody against p190A RhoGAP phosphorylated at Ser^{1150} was produced against the phosphopeptide Cys-Arg^{1145}-Gly-Arg-Lys-Val-phospho-Ser^{1150}-Ile-Val-Ser-Lys-Pro^{1155} by Biologica Co. (Nagoya, Japan). Y-27632, a Rho-kinase-specific inhibitor, was provided by Mitsubishi Pharma Co. (Osaka, Japan). ET-1, BQ-123, and BQ-788 were from Sigma. Other materials and chemicals were obtained from commercial sources.

Plasmid Constructs and Protein Purification—p190A RhoGAP fragments were amplified by PCR and subcloned into pGEX-2T (GE Healthcare, Princeton, NJ) or pEGFP-C1 (Clontech Laboratories, Mountain View, CA) plasmids, respectively. The cDNAs of p190A RhoGAP-4-S1150A, p190A RhoGAP-4-S1150A/T1173A/S1174A (p190A RhoGAP-4-AAA), p190A RhoGAP-4-S1150E/T1173E/S1174E (p190A RhoGAP-4-EEE), p190A RhoGAP-5-T1226A/S1236A (p190A RhoGAP-5-AA), p190A RhoGAP-5-T1226A/T1241A, p190A RhoGAP-full-length-S1150A (p190A RhoGAP-FL-S1150A), and p190A RhoGAP-FL-S1150E/T1173E/S1174E/T1226E/S1236E (p190A RhoGAP-FL-5E), in which Ala or Glu was substituted for Ser^{1150}, Thr^{1173}, Ser^{1174}, Thr^{1226}, Ser^{1236}, and/or Thr^{1241} were generated by site-directed mutagenesis. Rnd1 was isolated by PCR from a cDNA library and subcloned into pEF-BOS-HA plasmid. All fragments were confirmed by DNA sequencing. Glutathione *S*-transferase (GST) fusion proteins were produced in *Escherichia coli* BL21(DE3) and purified on glutathione-Sepharose 4B beads (GE Healthcare). GST-Rho-kinase-CAT (aa 6–553), a constitutively active form of Rho-kinase, and GST-p190A RhoGAP-4 + 5 (aa 953–1499) were produced in Sf9 cells with a baculovirus system and purified on glutathione-Sepharose 4B beads.

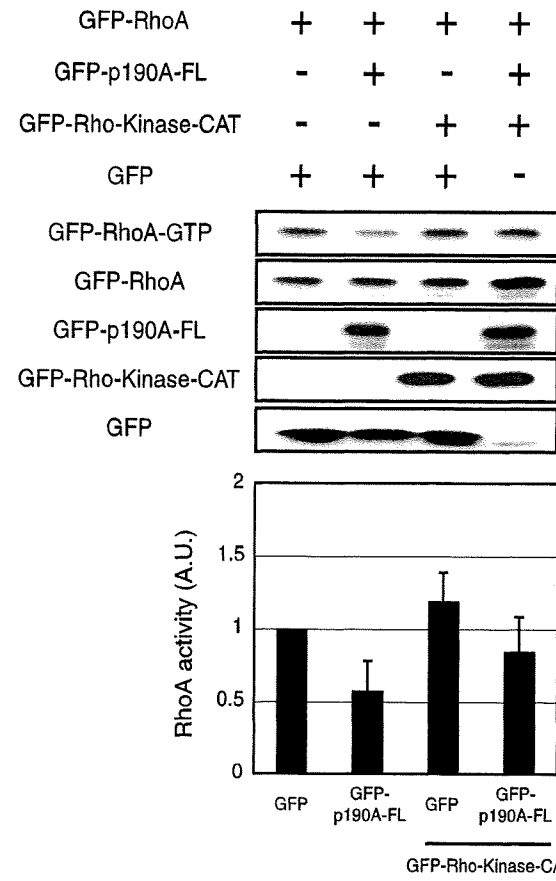

FIGURE 1. **Counteraction of p190A RhoGAP function by Rho-kinase in intact cells.** COS7 cells transfected with the indicated constructs were lysed with lysis buffer, and the lysates were incubated with GST-Rhotekin-RBD to precipitate the GTP-bound active form of RhoA. The eluates were analyzed by immunoblotting with anti-GFP Ab (*top*). The ratio of GFP-RhoA-GTP to total GFP-RhoA is shown (*bottom*). Data represent the means ± S.E. of four independent experiments.

Phosphorylation Assay—The phosphorylation assay was performed as previously described (25). In brief, the kinase reaction of Rho-kinase for p190A RhoGAP was carried out in 50 μl of the reaction mixture (50 mM Tris/HCl, pH 7.5, 1 mM EDTA, 1 mM EGTA, 1 mM dithiothreitol, 5 mM $MgCl_2$) containing 100 μM [γ-^{32}P]ATP (1–20 GBq/mmol), purified GST-Rho-kinase-CAT (0.001–0.1 μM), and 1 μM purified GST-p190A RhoGAP fragments. After incubation for 10 min at 30 °C, the reaction mixtures were boiled in SDS sample

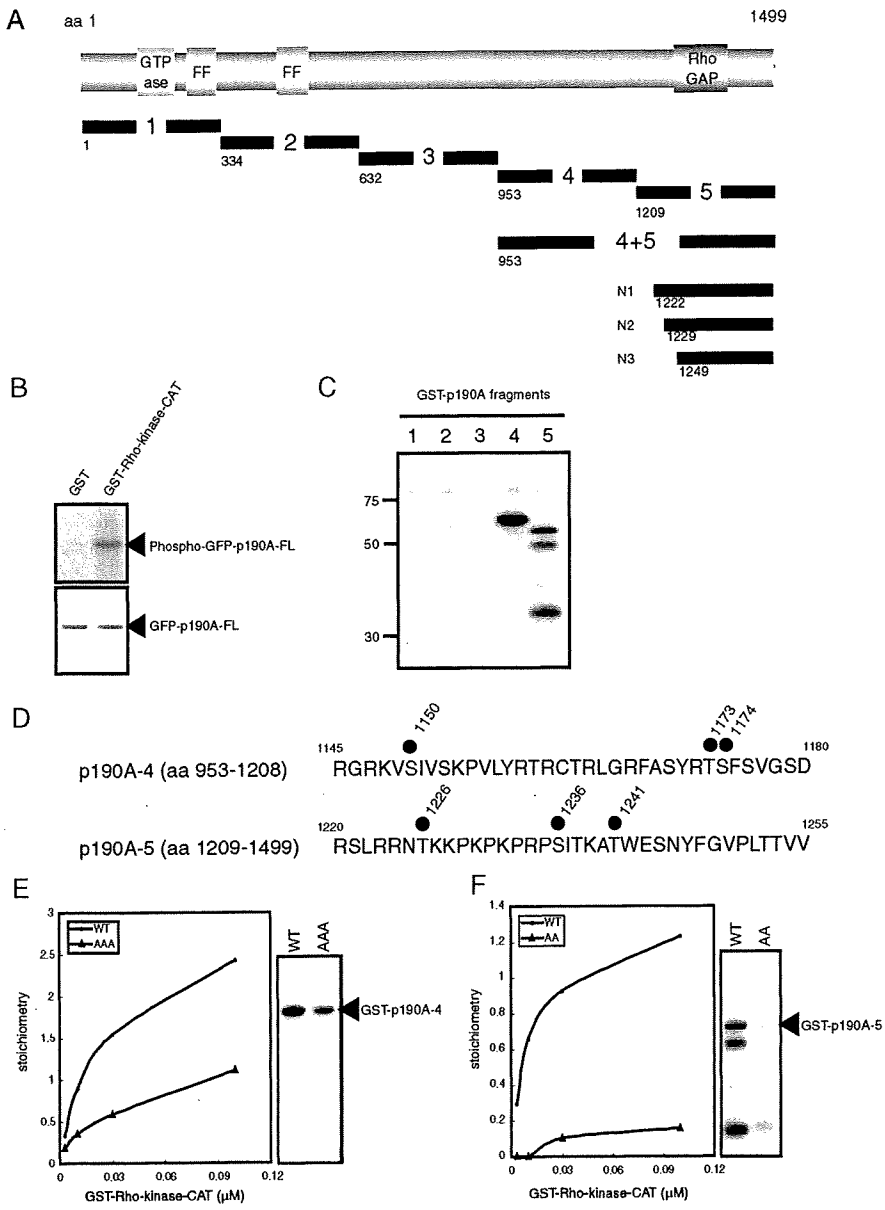

FIGURE 2. **Determination of phosphorylation sites of p190A RhoGAP by Rho-kinase.** *A*, schematic representation of domain structure and deletion constructs of p190A RhoGAP. *B*, immunoprecipitated GFP-p190A RhoGAP-FL from COS7 cell lysates was incubated with GST (*left*) or GST-Rho-kinase-CAT (*right*) and 100 μM [γ-^{32}P]ATP for 30 min at 30 °C. The reaction mixtures were subjected to SDS-PAGE and GFP-p190A RhoGAP was visualized by silver staining (*lower panel*). Phosphorylated proteins were imaged by autoradiography (*upper panel*). *C*, mapping of the region in p190A RhoGAP phosphorylated by Rho-kinase. The indicated GST-p190A RhoGAP fragments were phosphorylated by GST-Rho-kinase-CAT. The phosphorylated proteins were imaged by autoradiography. *D*, the phosphorylation sites of p190A RhoGAP are represented. Phosphorylated serine and threonine are in *red*. *E*, phosphorylation of GST-p190A RhoGAP-4-S1150A/T1173A/S1174A (*AAA*) by GST-Rho-kinase-CAT. *F*, phosphorylation of GST-p190A RhoGAP-5-T1226A/S1236A (*AA*) by GST-Rho-kinase-CAT. These results are representative of three independent experiments.

buffer and subjected to SDS-PAGE. The radiolabeled bands were visualized and estimated by an image analyzer (BAS2000, Fuji, Tokyo, Japan).

GAP Assay—The RhoA GAP assay was performed as previously described (26). Briefly, recombinant GST-RhoA was preloaded with 1 μM [γ-^{32}P]GTP (222 TBq/mmol, PerkinElmer Life Sciences) in 25 μl of buffer containing 50 mM HEPES, pH 7.4, 50 mM NaCl, 0.1 mM dithiothreitol, 0.1 mM EGTA, 5 mM EDTA, and 1 mg/ml bovine serum albumin for 10 min at 30 °C before the addition of $MgCl_2$ to a final concentration of 10 mM. An aliquot of [γ-^{32}P]GTP-loaded GST-RhoA was mixed with the GAP assay buffer, which contained 25 mM HEPES, pH 7.5, 50 mM NaCl, 1 mM $MgCl_2$, 0.1 mM dithiothreitol, 0.1 mM GTP, and 1 mg/ml bovine serum albumin in the presence of nonphosphorylated GST-p190A RhoGAP-4 + 5 or phosphorylated GST-p190A RhoGAP-4 + 5. The reaction was performed for 5 min at 30 °C and terminated by rapid addition of 5 ml of ice-cold buffer containing 50 mM HEPES, pH 7.5, 50 mM NaCl, and 1 mM $MgCl_2$. The samples were then immediately deposited onto nitrocellulose filters. The radioactivity retained on the filter was then subjected to quantitative analysis by scintillation counting. RhoGAP activity was detected as the remainder of [γ-^{32}P]GTP bound to GST-RhoA.

GTP-Rho Pulldown Assay—The activity of RhoA was determined by pulldown assay with the GST-Rho-binding domain of Rhotekin (GST-Rhotekin-RBD) as previously described (27). Briefly, the cells were washed with ice-cold phosphate-buffered saline and lysed in 500 μl of lysis buffer (50 mM Tris/HCl, pH 7.5, 1 mM EDTA, 10 mM $MgCl_2$, 500 mM NaCl, 0.5% Nonidet P-40, 0.1 mM (*p*-amidinophenyl)methanesulfonyl fluoride, 2.5 μg/ml aprotinin, 2.5 μg/ml leupeptin) containing 20 μg of GST-Rhotekin-RBD. The lysates were centrifuged at 20,000 × *g* for 3 min at 4 °C, and the supernatants were incubated with glutathione-Sepharose 4B beads for 30 min at 4 °C. The beads were washed with an excess of lysis buffer and then eluted with SDS-sample buffer. The eluates were subjected to SDS-PAGE, followed by immunoblot analysis with anti-GFP antibody or anti-RhoA antibody.

Rnd1-binding Assay—COS7 cells were transiently transfected with pEF-BOS-HA-Rnd1. The cells were washed with phosphate-buffered saline and lysed with lysis buffer (20 mM Tris/HCl, pH 7.5, 1 mM EDTA, 150 mM NaCl, 1 mM dithiothre-

itol, 1% Nonidet P-40, 0.2 μM Calyculin A, 1 mM sodium orthovanadate, 0.1 mM (*p*-amidinophenyl)methanesulfonyl fluoride, 2.5 μg/ml aprotinin, 2.5 μg/ml leupeptin). The lysates were centrifuged at 20,000 × *g* for 20 min at 4 °C, and the supernatants were incubated with glutathione-Sepharose 4B beads coated with 200 or 400 pmol of GST, 100 or 200 pmol of phosphorylated GST-p190A RhoGAP-4, and 100 or 200 pmol of nonphosphorylated GST-p190A RhoGAP-4 for 1 h at 4 °C. The beads were washed, and the eluates were subjected to SDS-PAGE, followed by immunoblot analysis with anti-HA antibody.

Cell Culture and Agonist Stimulation—Human aortic smooth muscle cells were obtained from Takara Bio Inc. (Shiga, Japan) and cultured in Dulbecco's modified Eagle's medium containing 10% fetal bovine serum, 100 units/ml penicillin, and 100 μg/ml streptomycin. Human aortic smooth muscle cells at the sixth passage were transfected with GFP-p190A RhoGAP-FL by using the Nucleofector system (Amaxa, Cologne, Germany). 24 h after transfection, the cells were starved for serum of 8 h and then stimulated with 1 μM ET-1. For the experiments with inhibitors, the cells were pretreated with inhibitors 30 min before ET-1 stimulation.

Measurement of Cell Size—To measure the cell size, human aortic smooth muscle cells were transfected with plasmids by using the Nucleofector system and then seeded on glass coverslips coated with fibronectin (BD Biosciences Pharmingen). 24 h after transfection, the cells were fixed with 3.0% formaldehyde in phosphate-buffered saline for 10 min and then treated with phosphate-buffered saline containing 0.1% Triton X-100 for 10 min. The cell area was measured with a laser scanning confocal microscope (model LSM510, Carl Zeiss, Oberkochene, Germany).

RESULTS

Counteraction of p190A RhoGAP Function by Rho-kinase—p190A and p190B RhoGAPs are ubiquitously expressed in various tissues and display GAP activity exclusively toward RhoA *in vivo* (28, 29). p190RhoGAP activity accounts for ~60% of the total RhoGAP activity detected in whole cell extracts in fibroblasts (30). Inhibition of p190RhoGAP activity is sufficient to promote RhoA activation in fibroblasts (30). Knockdown of p190A RhoGAP activity using siRNA increases RhoA activity in spreading microvascular endothelial cells (31). Thus, p190RhoGAP appears to account for the majority of RhoGAP activity.

Hence, we first examined whether Rho-kinase affects the p190A RhoGAP function in intact cells. GFP-RhoA was transfected into COS7 cells, and the amount of the GTP-bound form of GFP-RhoA was monitored by pulldown assay (Fig. 1). The expression of GFP-p190A RhoGAP-FL decreased the amount of GTP-bound GFP-RhoA in COS7 cells, suggesting that GFP-p190A RhoGAP-FL acts as RhoAGAP. The amount of GTP-bound GFP-RhoA was greater in the cells expressing GFP-p190A RhoGAP-FL and GFP-Rho-kinase-CAT than that in the cells expressing GFP-p190A RhoGAP-FL alone. This result suggests that Rho-kinase counteracts the GAP activity of p190A RhoGAP in COS7 cells.

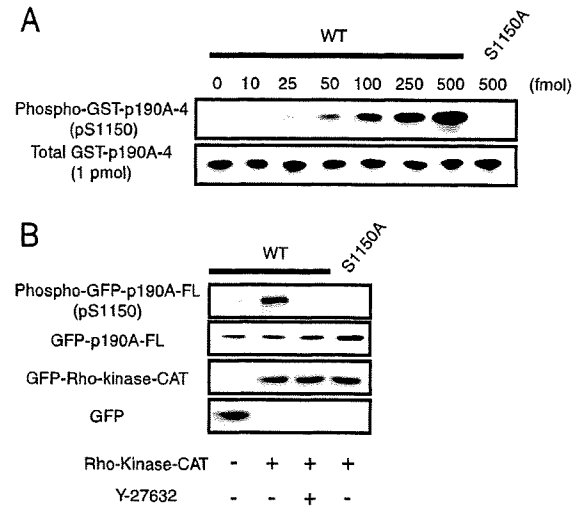

FIGURE 3. **Rho-kinase-dependent phosphorylation of p190A RhoGAP at Ser^{1150}.** *A*, specificity of the purified antibody against p190A RhoGAP phosphorylated at Ser^{1150}. One picomole of GST-p190A RhoGAP-4 containing the indicated amounts of phosphorylated GST-p190A RhoGAP-4-WT or -S1150A was subjected to SDS-PAGE, followed by immunoblot analysis with anti-p190A RhoGAP-pS1150 Ab (*upper panel*) or anti-GST Ab (*lower panel*). *B*, phosphorylation of p190A RhoGAP by Rho-kinase in intact cells. GFP-p190A RhoGAP-FL-WT or -S1150A was transiently transfected together with either GFP-Rho-kinase-CAT or GFP into COS7 cells as indicated. The transfected cells were treated with 20 μM Y-27632 or DMSO for the last 30 min of transfection. The cell lysates were analyzed by immunoblotting with anti-p190A RhoGAP-pS1150 Ab or anti-GFP Ab. These results are representative of three independent experiments.

In Vitro Phosphorylation of p190A RhoGAP by Rho-kinase—We then examined whether p190A RhoGAP is phosphorylated by Rho-kinase *in vitro*. To make a full length of p190A RhoGAP, we transiently transfected COS7 cells with GFP-p190A RhoGAP-FL, and immunoprecipitated GFP-p190A RhoGAP-FL from cell lysates with a polyclonal anti-GFP antibody. The immunoprecipitated GFP-p190A RhoGAP-FL was effectively phosphorylated by GST-Rho-kinase-CAT *in vitro* (Fig. 2*B*). We also found that Rho-kinase phosphorylated p190B RhoGAP (data not shown).

To determine the phosphorylation sites of p190A RhoGAP by Rho-kinase, p190A RhoGAP was divided into five fragments, including GST-p190A RhoGAP-1 (aa 1–333), p190A RhoGAP-2 (aa 334–637), p190A RhoGAP-3 (aa 632–952), p190A RhoGAP-4 (aa 953–1208), and p190A RhoGAP-5 (aa 1209–1499) (Fig. 2*A*). These fragments were produced from *E. coli* and then purified. GST-p190A RhoGAP-4 and p190A RhoGAP-5 were effectively phosphorylated by GST-Rho-kinase-CAT, whereas GST-p190A RhoGAP-1, GST-p190A RhoGAP-2, and GST-p190A RhoGAP-3 were not phosphorylated (Fig. 2*C*). To identify potential phosphorylation sites in p190A RhoGAP, liquid chromatography tandem mass spectrometry was performed and three potential phosphorylation sites in p190A RhoGAP-4 were identified, namely Ser^{1150}, Thr^{1173}, and Ser^{1174} (Fig. 2*D*). To determine the major phosphorylation sites, we substituted Ser^{1150}, Thr^{1173}, or Ser^{1174} with Ala to produce GST-p190A RhoGAP-4-S1150A, GST-p190A RhoGAP-4-T1173A, and GST-p190A RhoGAP-4-S1174A. However, the single Ala substitution did not affect the

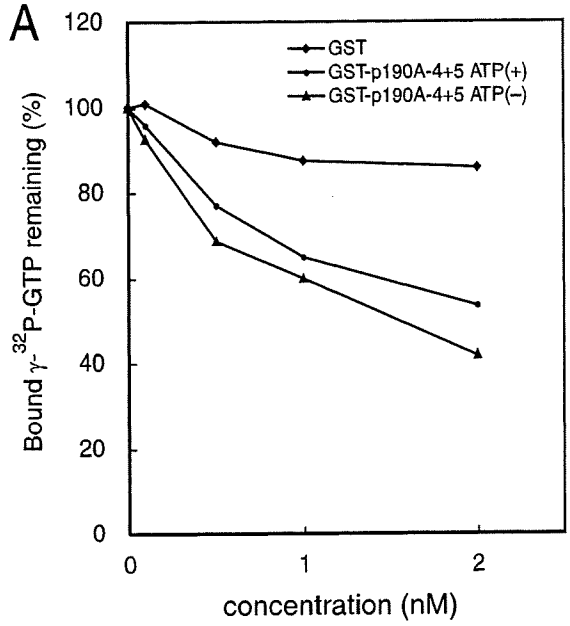

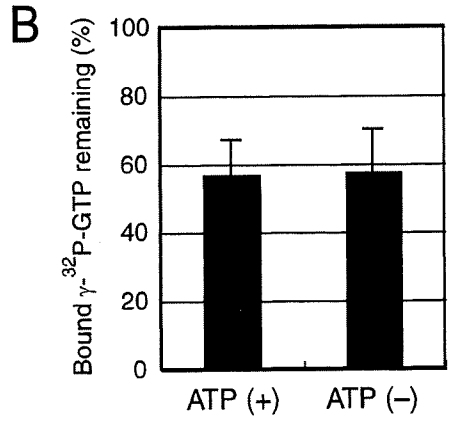

FIGURE 4. **Effect of phosphorylation of p190A RhoGAP by Rho-kinase on its GAP activity *in vitro*.** *A*, GST-p190A RhoGAP-4+5 was produced in Sf9 cells with a baculovirus system and purified on glutathione-Sepharose beads. Hydrolysis of GTP-bound GST-RhoA was monitored with GST (*squares*), nonphosphorylated GST-p190A RhoGAP-4+5 (*triangles*), or phosphorylated GST-p190A RhoGAP-4+5 (*circles*) for 5 min at 30 °C. The result is representative of three independent experiments. *B*, 1 μM [γ-^{32}P]GTP-bound GST-RhoA was incubated with 1 nM nonphosphorylated RhoGAP-4+5 or phosphorylated GST-p190A RhoGAP-4+5 for 5 min at 30 °C. Data are indicated as mean ± S.D. (n = 20, respectively, p = 0.82).

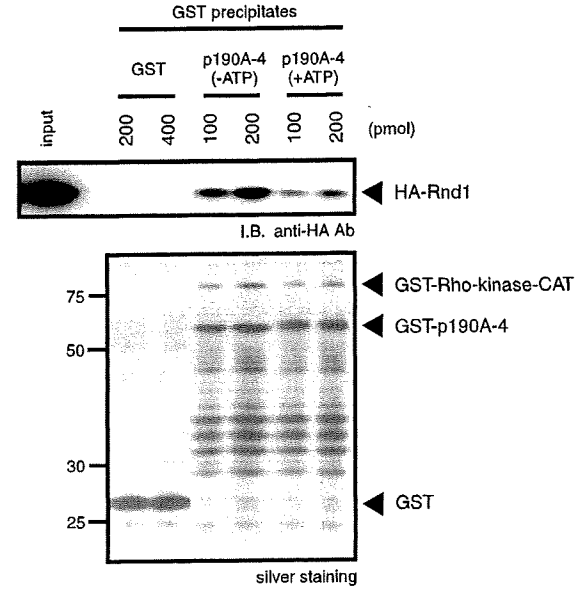

FIGURE 5. **Binding of p190A RhoGAP to Rnd1.** COS7 cells were transiently transfected with pEF-BOS-HA-Rnd1. The cell lysates were incubated with glutathione-Sepharose 4B beads coated with 200 or 400 pmol of GST, 100 or 200 pmol of phosphorylated GST-p190A RhoGAP-4, and 100 or 200 pmol of nonphosphorylated GST-p190A RhoGAP-4 for 1 h at 4 °C. The beads were washed, and the eluates were subjected to SDS-PAGE, followed by immunoblot analysis with anti-HA Ab. GST fusion proteins were visualized by silver staining. The result is representative of three independent experiments.

phosphorylation efficiency (data not shown). Then, Ser^{1150}, Thr^{1173}, and Ser^{1174} were simultaneously substituted with Ala to produce GST-p190A RhoGAP-4-S1150A/T1173A/S1174A (GST-p190A RhoGAP-4-AAA). The phosphorylation efficiency of GST-p190A RhoGAP-4-AAA was substantially reduced compared with the wild type (Fig. 2*E*), suggesting that at least two potential phosphorylation sites among these three sites are efficient phosphorylation sites.

The phosphorylation sites in p190A RhoGAP-5 were not identified by liquid chromatography tandem mass spectrometry. To identify potential phosphorylation sites in p190A RhoGAP-5, we produced the additional deletion mutants, including GST-p190A RhoGAP-ΔN1 (aa 1222–1499), p190A RhoGAP-ΔN2 (aa 1229–1499), and p190A RhoGAP-ΔN3 (aa 1249–1499) (Fig. 2*A*). GST-p190A RhoGAP-ΔN1 was highly phosphorylated and GST-p190A RhoGAP-ΔN2 was intermediately phosphorylated by GST-Rho-kinase-CAT, whereas GST-p190A RhoGAP-ΔN3 was not phosphorylated (supplemental Fig. S1*A*), suggesting that phosphorylation sites exist in aa 1222–1228 and aa 1229–1248. Because (R/K)*XX*(S/T) or (R/K)*X*(S/T) (X is any amino acid) is the consensus phosphorylation sequence by Rho-kinase, the potential phosphorylation sites in p190A-5 are Thr^{1226} in aa 1222–1228, and Ser^{1236} and Thr^{1241} in aa 1229–1248 (Fig. 2*D*), suggesting that Thr^{1226} is the putative major phosphorylation site. To determine the major phosphorylation sites in p190A RhoGAP-5, we produced GST-p190A RhoGAP-5-T1226A/S1236A (GST-p190A RhoGAP-5-AA) and GST-p190A RhoGAP-5-T1226A/T1241A. GST-p190A RhoGAP-5-AA was minimally phosphorylated by GST-Rho-kinase-CAT (Fig. 2*F*). The degree of phosphorylation of GST-p190A RhoGAP-5-T1226A/T1241A by GST-Rho-kinase-CAT was approximately half (supplemental Fig. S1*B*). Taken together, these results suggest that Rho-kinase phosphorylates p190A RhoGAP presumably at a minimum of five sites, including Ser^{1150}, Thr^{1173}, Ser^{1174}, Thr^{1226}, and Ser^{1236} *in vitro*.

In Vivo Phosphorylation of p190A RhoGAP by Rho-kinase—To examine the phosphorylation state of p190A RhoGAP by Rho-kinase *in vivo*, we prepared rabbit polyclonal antibodies that specifically recognize p190A RhoGAP phosphorylated at respective phosphorylation sites. Among them, the anti-p190A RhoGAP-pS1150 antibody specifically recognized GST-p190A

Phosphorylation of p190A RhoGAP by Rho-kinase

RhoGAP-4 phosphorylated by GST-Rho-kinase-CAT in a dose-dependent manner, but not phosphorylated GST-p190A RhoGAP-4-S1150A (Fig. 3*A*), indicating that the antibody specifically recognized GST-p190A RhoGAP-4 that was phosphorylated at Ser^{1150}. The anti-p190A RhoGAP-pT1173 and pS1174 antibodies only slightly recognized phosphorylated p190A RhoGAP, suggesting that Thr^{1173} and Ser^{1174} are not major phosphorylation sites. Alternatively, these antibodies did not work well on phosphorylated p190A RhoGAP, although they recognized the antigen phosphopeptides (data not shown). The anti-p190A RhoGAP-pT1226 and -pS1236 antibodies could recognize the phosphorylated p190A RhoGAP *in vitro* in a manner similar to that of anti-p190A RhoGAP-pS1150 antibody (data not shown).

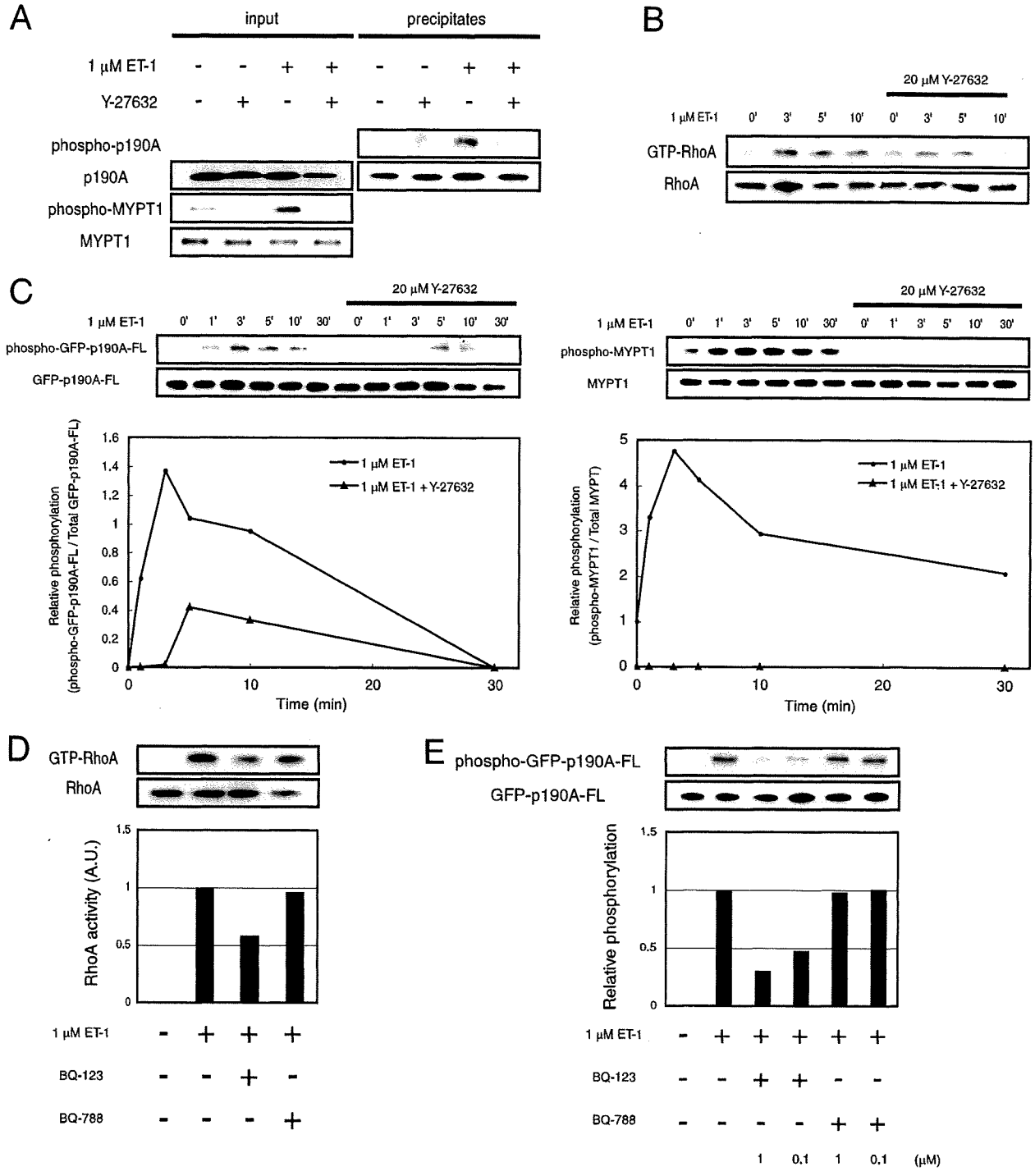

To examine whether Rho-kinase phosphorylates p190A RhoGAP in intact cells, GFP-p190A RhoGAP-FL was exogenously co-transfected with GFP-Rho-kinase-CAT into COS7 cells. Co-transfection of Rho-kinase-CAT resulted in an increase of phosphorylated GFP-p190A RhoGAP-FL at Ser^{1150} (Fig. 3*B*). Treatment of the cells with Y-27632 inhibited phosphorylation of GFP-p190A RhoGAP-FL by GFP-Rho-kinase-CAT. GFP-Rho-kinase-CAT failed to phosphorylate GFP-p190A RhoGAP-FL-S1150A. Under the same conditions, phosphorylation of endogenous p190A RhoGAP at Ser^{1150} was not detected, presumably because the expression level of p190A RhoGAP was low in COS7 cells. Taken together, these results indicate that Rho-kinase can phosphorylate p190A RhoGAP at Ser^{1150} in COS7 cells. Similarly, the immunoblot analysis, through the use of the anti-p190A RhoGAP-pT1226 and -pS1236 antibodies, revealed that Rho-kinase can phosphorylate p190A RhoGAP at Thr^{1226} and Ser^{1236} in COS7 cells (data not shown).

Effects of Phosphorylation of p190A RhoGAP by Rho-kinase on Its GAP Activity—Does phosphorylation of p190A RhoGAP by Rho-kinase affect p190A RhoGAP functions? To examine the effects of phosphorylation on the GAP activity of p190A RhoGAP, we tried to produce and purify the full length of p190A RhoGAP from *E. coli* and insect cells, but the procedure failed. We then prepared nonphosphorylated and phosphorylated GST-p190A RhoGAP-4+5, which includes the identified five phosphorylation sites and the RhoGAP catalytic domain, and performed an *in vitro* GAP assay. Hydrolysis of GTP-bound GST-RhoA was accelerated by using purified GST-p190A RhoGAP-4+5 in a dose-dependent and time-dependent manner (supplemental Fig. S2). The GAP activity of GFP-p190A RhoGAP-4+5 was not dramatically affected by phosphorylation (Fig. 4, *A* and *B*).

We here found that Rho-kinase appeared to inhibit the p190A RhoGAP activity in COS7 cells (Fig. 1). How does Rho-kinase regulate the GAP activity of p190A RhoGAP in intact cells? Small GTPase Rnd is a member of the distinct subgroup of the Rho family GTPases and regulates the organization of actin cytoskeleton (32). Expression of Rnd inhibits the formation of the stress fibers in response to lysophosphatidic acid stimulation in fibroblasts (33), suggesting that Rnd antagonizes the action of RhoA. Consistently, Rnd binds to p190A RhoGAP and increases its GAP activity toward GTP-bound RhoA, resulting in RhoA inactivation (34, 35). This observation prompted us to examine whether phosphorylation of p190A RhoGAP affects its interaction with Rnd1. HA-Rnd1 efficiently interacted with GST-p190A RhoGAP-4 in the pulldown assay, and phosphorylation of GST-p190A RhoGAP-4 by Rho-kinase attenuated its interaction with Rnd1 (Fig. 5). Thus, it is conceivable that Rho-kinase suppresses the GAP activity of p190A RhoGAP by inhibiting the interaction with Rnd1 through phosphorylation.

Phosphorylation of p190A RhoGAP in Cultured Vascular Smooth Muscle Cells—To understand the physiological functions of p190A RhoGAP, we confirmed the expression profile of p190A RhoGAP in various rat tissues and found that p190A RhoGAP was highly expressed in brain, lung, and aorta (supplemental Fig. S3*A*). We also found that p190A RhoGAP was highly expressed in primary human aortic smooth muscle and endothelial cells (supplemental Fig. S3*B*).

Then, we monitored phosphorylation of endogenous p190A RhoGAP in human aortic smooth muscle cells. The basal phosphorylation level of p190A RhoGAP at Ser^{1150} was not detected (Fig. 6*A*). ET-1 is known to activate the Rho/Rho-kinase pathway (17). Stimulation of smooth muscle cells by ET-1 induced phosphorylation of endogenous p190A RhoGAP at Ser^{1150} (Fig. 6*A*). Treatment of the cells with Y-27632 inhibited ET-1-induced phosphorylation of p190A RhoGAP. As a positive control, the MYPT1 phosphorylation level was monitored. Phosphorylation of MYPT1 at Thr^{853} decreases the activity of myosin phosphatase in vascular smooth muscle cells: this phosphorylation is used as an indicator of the activity of Rho-kinase (17). ET-1 induced phosphorylation of MYPT1 at Thr^{853}, whereas Y-27632 completely inhibited this phosphorylation. Taken together, these results suggest that ET-1 provoked phosphorylation of endogenous p190A RhoGAP at Ser^{1150} in a Rho-kinase dependent fashion in cultured vascular smooth muscle cells.

Of note, the immunoblot analysis using the anti-p190A RhoGAP-pT1226 and -pS1236 antibodies revealed that p190A RhoGAP was phosphorylated upon treatment with ET-1, but these phosphorylations were not dramatically inhibited by Y-27632, suggesting that these sites are not major phosphorylation sites by Rho-kinase in aortic smooth muscle cells (data not shown).

A high concentration of ET-1 has been shown to induce activation of Rho/Rho-kinase and subsequent MYPT1 phosphorylation, thereby resulting in the sustained contraction of vascular

FIGURE 6. **Phosphorylation of p190A RhoGAP by Rho-kinase in cultured vascular smooth muscle cells.** *A*, phosphorylation of endogenous p190A RhoGAP in cultured vascular smooth muscle cells. The cells were incubated with 20 μM Y-27632 or DMSO for 30 min, and then treated with 1 μM ET-1 for 3 min. Endogenous p190A RhoGAP was immunoprecipitated with anti-p190A RhoGAP Ab (Upstate). The amounts of phosphorylated p190A RhoGAP were determined by immunoblot analysis with anti-p190A RhoGAP-pS1150 Ab. The amounts of phosphorylated and total MYPT1 were examined as a positive control. *B*, effect of Rho-kinase-specific inhibitor on ET-1-induced sustained RhoA activation. After serum depletion for 8 h, the cells were incubated with 20 μM Y-27632 or DMSO for 30 min, and then stimulated with 1 μM ET-1 for the indicated periods of time. The cells were lysed with lysis buffer, and the lysates were incubated with GST-Rhotekin-RBD to precipitate the GTP-bound active form of RhoA. The eluates were analyzed by immunoblotting with anti-RhoA Ab. *C*, ET-1-induced sustained phosphorylation of p190A RhoGAP in cultured vascular smooth muscle cells. The cells were transiently transfected with GFP-p190A RhoGAP-FL with the use of the Nucleofector system. After serum depletion for 8 h, the cells were incubated with 20 μM Y-27632 or DMSO for 30 min, and then stimulated with 1 μM ET-1 for the indicated periods of time. The cell lysates were subjected to SDS-PAGE followed by immunoblot analysis with anti-p190A RhoGAP-pS1150 Ab, anti-p190A RhoGAP Ab (Pharmingen), anti-MYPT1-pT853 Ab, and anti-MYPT1 Ab. *D*, effect of ET-1 antagonists on RhoA activity. The cells were starved for serum of 8 h and then stimulated with 1 μM ET-1 for 3 min after treatment with 1 μM BQ-123 or 1 μM BQ-788 for 30 min. The cells were lysed with lysis buffer, and the lysates were incubated with GST-Rhotekin-RBD to precipitate the GTP-bound active form of RhoA. The eluates were analyzed by immunoblotting with anti-RhoA Ab (*top*). The ratio of GTP-RhoA to total RhoA is shown (*bottom*). *E*, effect of ET antagonists on phosphorylation of p190A RhoGAP. The cells were transiently transfected with GFP-p190A RhoGAP-FL. Twenty-four hours after transfection, the cells were starved for serum of 8 h and then stimulated with 1 μM ET-1 for 3 min after treatment with BQ-123 (1 μM, 0.1 μM) or BQ-788 (1 μM, 0.1 μM) for 30 min. The cell lysates were subjected to immunoblot analysis with anti-p190A RhoGAP-pS1150 Ab and anti-p190A RhoGAP Ab (Pharmingen). These results are representative of three independent experiments.

The Journal of Biological Chemistry ASBMB

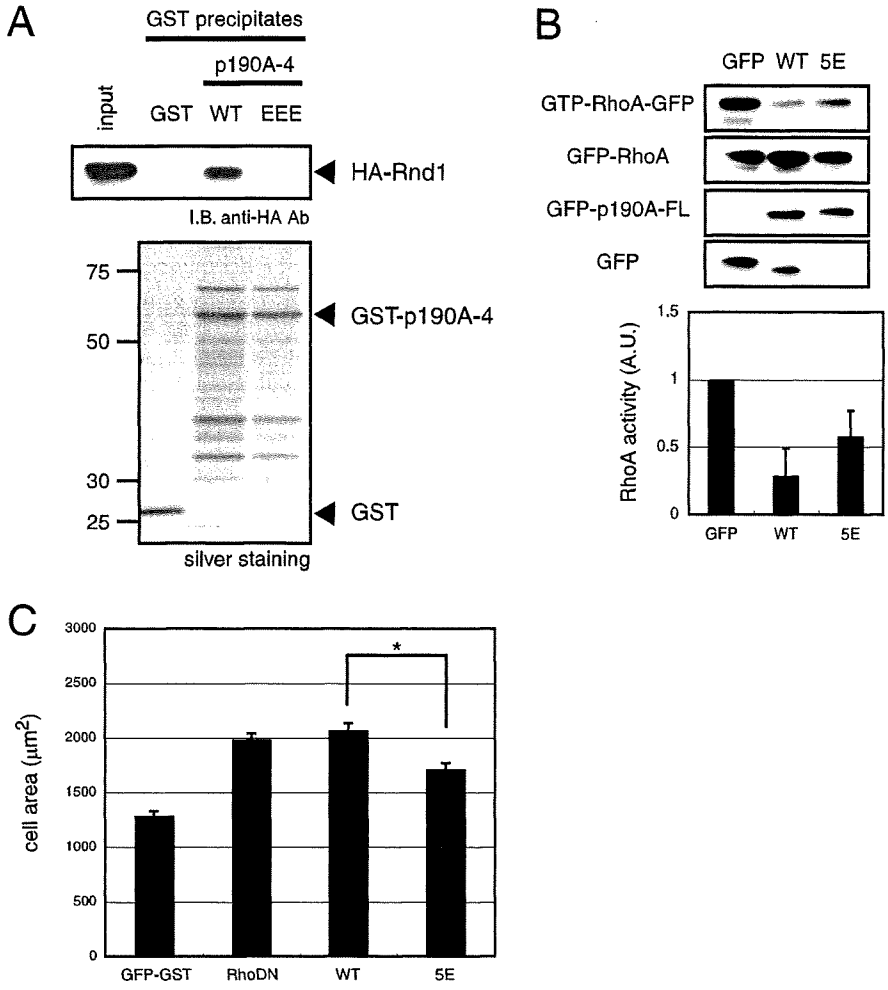

FIGURE 7. **Effects of phosphomimic mutation of p190A RhoGAP.** *A*, binding of phosphomimic mutant to Rnd1. COS7 cells were transiently transfected with pEF-BOS-HA-Rnd1. The cell lysates were incubated with glutathione-Sepharose 4B beads coated with 200 pmol of GST, GST-p190A RhoGAP-4-WT, and GST-p190A RhoGAP-4-EEE for 1 h at 4 °C. The beads were washed, and the eluates were subjected to SDS-PAGE, followed by immunoblot analysis with anti-HA Ab. GST fusion proteins were visualized by silver staining. The result is representative of three independent experiments. *B*, effect of GFP-p190A RhoGAP-FL-5E on RhoA in COS7 cells. The activity of RhoA was monitored by pulldown assay with the GST-Rhotekin-RBD. The eluates were analyzed by immunoblotting with anti-GFP Ab (*top*). The ratio of GFP-RhoA-GTP to total GFP-RhoA is shown (*bottom*). Data represent the means ± S.E. of four independent experiments. *C*, effect of phosphomimic mutant of p190A RhoGAP on vascular smooth muscle cell size. The area of cells transfected with the indicated constructs was measured. Data are indicated as mean ± S.D. ($n > 100$ in each experiment), and these results are representative of three independent experiments. The *asterisk* indicates a significant difference ($p < 0.01$) from the value of GFP-p190A RhoGAP-FL-WT.

smooth muscle (17). We found that a high concentration of ET-1 induced sustained RhoA activation (supplemental Fig. S4), whereas Y-27632 suppressed ET-1-induced sustained RhoA activation (Fig. 6*B* and supplemental Fig. S4), suggesting that Rho-kinase is involved in prolonged RhoA activation.

Because the sensitivity of the anti-p190A RhoGAP-pS1150 antibody is relatively low, we transiently transfected cultured vascular smooth muscle cells with GFP-p190A RhoGAP-FL to examine whether ET-1 induces sustained phosphorylation of p190A RhoGAP in a Rho/Rho-kinase-dependent manner (Fig. 6*C*). ET-1 induced sustained phosphorylation of GFP-p190A RhoGAP-FL at Ser^{1150}, and Y-27632 effectively inhibited ET-1-induced phosphorylation of GFP-p190A RhoGAP-FL. Under the same conditions, ET-1 induced sustained phosphorylation of MYPT1 at Thr^{853}, whereas Y-27632 completely inhibited this phosphorylation (Fig. 6*C*). Other vasoconstrictors such as angiotensin II, acetylcholine, and thrombin slightly induced phosphorylation of p190A RhoGAP (data not shown). These results suggest that ET-1 induces sustained phosphorylation of p190A RhoGAP at Ser^{1150} in a Rho/Rho-kinase-dependent manner in cultured vascular smooth muscle cells.

There are three different types of ET receptors, ET_A, ET_B, and ET_C. ET_B receptors are classified into two subtypes, ET_{B1} and ET_{B2}. ET_A and ET_{B2} receptors are expressed in vascular smooth muscle, and both receptors mediate vascular smooth muscle contraction (36). To examine which types of ET receptors are involved in phosphorylation of p190A RhoGAP, vascular smooth muscle cells transfected with GFP-p190A RhoGAP-FL were treated with a selective ET_A or ET_B antagonist. BQ-123, a selective ET_A antagonist, inhibited ET-1-induced RhoA activation and phosphorylation of p190A RhoGAP, whereas BQ-788, a selective ET_B antagonist, minimally affected ET-1-induced RhoA activation and phosphorylation of p190A RhoGAP (Fig. 6, *D* and *E*). These results suggest that ET-1 induces p190A RhoGAP phosphorylation via RhoA activation through ET_A receptor in cultured vascular smooth muscle cells.

Because the activity of p190A RhoGAP is thought to be regulated through the tyrosine phosphorylation by Src family kinases and Abl family kinases, we examined whether ET-1 affects the tyrosine phosphorylation state of p190A RhoGAP. Sodium orthovanadate, an inhibitor of phosphotyrosine phosphatase, increased the tyrosine phosphorylation level of GFP-190A RhoGAP-FL. Under the same condition, ET-1 did not induce the tyrosine phosphorylation of p190A RhoGAP (supplemental Fig. S5). These results suggest that ET-1 did not induce the tyrosine phosphorylation of p190A RhoGAP in cultured vascular smooth muscle cells.

Effect of Phosphomimic Mutant of p190A RhoGAP on Vascular Smooth Muscle Cell Size—To explore the effect of phosphorylation of p190A RhoGAP *in vitro*, we replaced three putative phosphorylation sites in p190A RhoGAP-4 with Glu to produce

GST-p190A RhoGAP-4-EEE, the phosphomimic mutants. We first examined the effect of the Glu substitution on Rnd1 binding to p190A RhoGAP. HA-Rnd1 associated with GST-p190A RhoGAP-4-WT in the pulldown assay, whereas it associated less efficiently with GST-p190A RhoGAP-4-EEE (Fig. 7*A*), suggesting that the Glu substitution weakens the binding of Rnd1 to p190A RhoGAP.

We next replaced five putative phosphorylation sites with Glu to produce GFP-p190A RhoGAP-FL-5E to examine the effect of phosphorylation of p190A RhoGAP on RhoA in intact cells. We found that the amount of GTP-bound GFP-RhoA was greater in the cells expressing GFP-p190A RhoGAP-FL-5E than that in the cells expressing GFP-p190A RhoGAP-WT, suggesting that GFP-p190A RhoGAP-5E shows a weaker GAP activity than wild type (Fig. 7*B*).

It was previously demonstrated that the constitutively active form of RhoA (RhoA Val^{14}) induces the formation of stress fibers and decreases the size of vascular smooth muscle cells through contraction, whereas the dominant negative form of RhoA (RhoA Asn^{19}) weakens the formation of stress fibers and increases the cell size (37). We employed this assay to compare the effects of p190A RhoGAP and GFP-p190A RhoGAP-FL-5E on cell contraction. The vascular smooth muscle cells were transiently transfected with GFP-RhoA Asn^{19} or GFP-p190A RhoGAP-FL-WT, and the cell sizes were measured. The expression of GFP-p190A RhoGAP-FL-WT increased the cell size under these conditions, with GFP-RhoA Asn^{19} showing increased cell size (Fig. 7*C*), suggesting that basal RhoA activity is necessary for maintaining cell contractility. GFP-p190A RhoGAP-FL-5E showed a weaker effect than that of GFP-p190A RhoGAP-FL-WT ($p < 0.01$), suggesting that the GFP-p190A RhoGAP-FL-5E mutant mimics the phosphorylation state and shows weaker activity to inactivate RhoA.

DISCUSSION

Here we show that Rho-kinase phosphorylated p190A RhoGAP in a cell-free system and identified putative phosphorylation sites, including Ser^{1150}. Rho-kinase phosphorylated p190A RhoGAP at Ser^{1150} in intact cells. Phosphorylation by Rho-kinase of the p190A RhoGAP fragment containing the GAP domain did not affect GAP activity toward RhoA in a cell-free system. However, we found that constitutively active Rho-kinase could counteract p190A RhoGAP activity in intact cells. The binding of Rnd to p190A RhoGAP is thought to enhance its GAP activity (35). Phosphorylation of p190A RhoGAP by Rho-kinase inhibited its binding to Rnd. The phosphomimic mutant of p190A RhoGAP showed the weaker Rnd binding and RhoGAP activities. Thus, it is conceivable that Rho-kinase phosphorylates p190A RhoGAP and thereby inhibits its binding to Rnd, resulting in inactivation of p190A RhoGAP and subsequent prolonged RhoA activation.

The primary action of ET-1 *in vivo* is to increase blood pressure and vascular tone. ET-1 was shown to activate Gq/G13, and to induce Ca^{2+} mobilization and subsequent phosphorylation of myosin light chain in cultured aortic smooth muscle cells (38). High concentrations of ET-1 cause long-lasting vasoconstriction (17). The transient contractile phase is mediated by G_q and Ca^{2+}/calmodulin-dependent activation of myosin light chain kinase (39). On the other hand, the sustained phase is mediated by G_{13}-dependent activation of the Rho/Rho-kinase signaling pathway (39). Consistently, high concentrations of ET-1 transiently induce Ca^{2+} mobilization in smooth muscle cells, which lasts for a minute (17).

Here we show that high concentrations of ET-1 induced sustained RhoA activation and p190RhoGAP phosphorylation in cultured vascular smooth muscle cells under the conditions in which ET-1 induced sustained MYPT1 phosphorylation. Y-27632 inhibited ET-1-induced phosphorylation of MYPT-1 as well as p190A RhoGAP and partly prohibited sustained RhoA activation, suggesting that ET-1 causes prolonged activation of the RhoA/Rho-kinase pathway. We also found that expression of p190A RhoGAP weakens the cell contractility, whereas the phosphomimic 5E mutant showed weaker activity than that of the wild type. Thus, it is possible that ET-1 induces the Rho/Rho-kinase activation and subsequent phosphorylation of p190A RhoGAP, thereby constituting the positive feedback loop to amplify Rho activation and promote contraction of vascular smooth muscle cells. ET-1 is thought to be involved in the pathogenesis of various cardiovascular diseases such as essential hypertension, pulmonary hypertension, and coronary vasospastic angina (40). The next challenge will be to explore whether p190A RhoGAP phosphorylation participates in these cardiovascular diseases.

Acknowledgments—We are grateful for Dr. T. Itoh (Nagoya City University), members of Kaibuchi Laboratory, especially Dr. T. Watanabe and Dr. T. Hikita for helpful discussion, and T. Ishii for secretarial assistance.

REFERENCES

1. Burridge, K., and Wennerberg, K. (2004) *Cell* **116,** 167–179
2. Jaffe, A. B., and Hall, A. (2005) *Annu. Rev. Cell Dev. Biol.* **21,** 247–269
3. Hartshorne, D. J., Ito, M., and Erdodi, F. (2004) *J. Biol. Chem.* **279,** 37211–37214
4. Ito, M., Nakano, T., Erdodi, F., and Hartshorne, D. J. (2004) *Mol. Cell Biochem.* **259,** 197–209
5. Matsumura, F., and Hartshorne, D. J. (2008) *Biochem. Biophys. Res. Commun.* **369,** 149–156
6. Somlyo, A. P., and Somlyo, A. V. (2003) *Physiol. Rev.* **83,** 1325–1358
7. Lemmon, M. A., and Ferguson, K. M. (2000) *Biochem. J.* **350,** 1–18
8. Rossman, K. L., Cheng, L., Mahon, G. M., Rojas, R. J., Snyder, J. T., Whitehead, I. P., and Sondek, J. (2003) *J. Biol. Chem.* **278,** 18393–18400
9. Kozasa, T., Jiang, X., Hart, M. J., Sternweis, P. M., Singer, W. D., Gilman, A. G., Bollag, G., and Sternweis, P. C. (1998) *Science* **280,** 2109–2111
10. Fukuhara, S., Murga, C., Zohar, M., Igishi, T., and Gutkind, J. S. (1999) *J. Biol. Chem.* **274,** 5868–5879
11. Suzuki, N., Nakamura, S., Mano, H., and Kozasa, T. (2003) *Proc. Natl. Acad. Sci. U. S. A.* **100,** 733–738
12. Sternweis, P. C., Carter, A. M., Chen, Z., Danesh, S. M., Hsiung, Y. F., and Singer, W. D. (2007) *Adv. Protein Chem.* **74,** 189–228
13. Bernards, A., and Settleman, J. (2004) *Trends Cell Biol.* **14,** 377–385
14. Tcherkezian, J., and Lamarche-Vane, N. (2007) *Biol. Cell* **99,** 67–86
15. Sakurada, S., Okamoto, H., Takuwa, N., Sugimoto, N., and Takuwa, Y. (2001) *Am. J. Physiol. Cell* **281,** C571–C578
16. Arthur, W. T., and Burridge, K. (2001) *Mol. Biol. Cell* **12,** 2711–2720
17. Woodsome, T. P., Polzin, A., Kitazawa, K., Eto, M., and Kitazawa, T. (2006) *J. Cell Sci.* **119,** 1769–1780
18. Loirand, G., Guerin, P., and Pacaud, P. (2006) *Circulation Res.* **98,** 322–334
19. Wettschureck, N., and Offermanns, S. (2002) *J. Mol. Med. (Berlin)* **80,** 629–638

20. Moriki, N., Ito, M., Seko, T., Kureishi, Y., Okamoto, R., Nakakuki, T., Kongo, M., Isaka, N., Kaibuchi, K., and Nakano, T. (2004) *Hypertens. Res.* **27,** 263–270
21. Kandabashi, T., Shimokawa, H., Miyata, K., Kunihiro, I., Kawano, Y., Fukata, Y., Higo, T., Egashira, K., Takahashi, S., Kaibuchi, K., and Takeshita, A. (2000) *Circulation* **101,** 1319–1323
22. Sato, M., Tani, E., Fujikawa, H., and Kaibuchi, K. (2000) *Circ. Res.* **87,** 195–200
23. Guilluy, C., Sauzeau, V., Rolli-Derkinderen, M., Guerin, P., Sagan, C., Pacaud, P., and Loirand, G. (2005) *Br. J. Pharmacol.* **146,** 1010–1018
24. Kimura, K., Fukata, Y., Matsuoka, Y., Bennett, V., Matsuura, Y., Okawa, K., Iwamatsu, A., and Kaibuchi, K. (1998) *J. Biol. Chem.* **273,** 5542–5548
25. Amano, M., Ito, M., Kimura, K., Fukata, Y., Chihara, K., Nakano, T., Matsuura, Y., and Kaibuchi, K. (1996) *J. Biol. Chem.* **271,** 20246–20249
26. Ligeti, E., and Settleman, J. (2006) *Methods Enzymol.* **406,** 104–117
27. Ren, X. D., Kiosses, W. B., and Schwartz, M. A. (1999) *EMBO J.* **18,** 578–585
28. Ridley, A. J., Self, A. J., Kasmi, F., Paterson, H. F., Hall, A., Marshall, C. J., and Ellis, C. (1993) *EMBO J.* **12,** 5151–5160
29. Settleman, J., Narasimhan, V., Foster, L. C., and Weinberg, R. A. (1992) *Cell* **69,** 539–549
30. Vincent, S., and Settleman, J. (1999) *Eur. J. Cell Biol.* **78,** 539–548
31. Mammoto, A., Huang, S., and Ingber, D. E. (2007) *J. Cell Sci.* **120,** 456–467
32. Chardin, P. (2006) *Nat. Rev. Mol. Cell. Biol.* **7,** 54–62
33. Nobes, C. D., Lauritzen, I., Mattei, M. G., Paris, S., Hall, A., and Chardin, P. (1998) *J. Biol. Chem.* **141,** 187–197
34. Harada, A., Katoh, H., and Negishi, M. (2005) *J. Biol. Chem.* **280,** 18418–18424
35. Wennerberg, K., Forget, M. A., Ellerbroek, S. M., Arthur, W. T., Burridge, K., Settleman, J., Der, C. J., and Hansen, S. H. (2003) *Curr. Biol.* **13,** 1106–1115
36. Hynynen, M. M., and Khalil, R. A. (2006) *Recent Patents Cardiovasc. Drug Discov.* **1,** 95–108
37. Worth, N. F., Campbell, G. R., Campbell, J. H., and Rolfe, B. E. (2004) *Cell Motil. Cytoskeleton* **59,** 189–200
38. Gohla, A., Schultz, G., and Offermanns, S. (2000) *Circ. Res.* **87,** 221–227
39. Hersch, E., Huang, J., Grider, J. R., and Murthy, K. S. (2004) *Am. J. Physiol.* **287,** C1209–C1218
40. Agapitov, A. V., and Haynes, W. G. (2002) *J. Renin Angiotensin Aldosterone Syst.* **3,** 1–15

Published July 13, 2009

ARTICLE

Mobile DHHC palmitoylating enzyme mediates activity-sensitive synaptic targeting of PSD-95

Jun Noritake,[1] Yuko Fukata,[1,2] Tsuyoshi Iwanaga,[1] Naoki Hosomi,[3] Ryouhei Tsutsumi,[1] Naoto Matsuda,[1] Hideki Tani,[4] Hiroko Iwanari,[3] Yasuhiro Mochizuki,[3] Tatsuhiko Kodama,[3] Yoshiharu Matsuura,[4] David S. Bredt,[5] Takao Hamakubo,[3] and Masaki Fukata[1,2]

[1]Division of Membrane Physiology, Department of Cell Physiology, National Institute for Physiological Sciences, Okazaki, Aichi 444-8787, Japan
[2]Precursory Research for Embryonic Science and Technology, Japan Science and Technology Agency, Chiyoda-ku, Tokyo 102-0075, Japan
[3]Laboratory for Systems Biology and Medicine, Research Center for Advanced Science and Technology, The University of Tokyo, Meguro-ku, Tokyo 153-8904, Japan
[4]Department of Molecular Virology, Research Institute for Microbial Diseases, Osaka University, Suita, Osaka 565-0871, Japan
[5]Department of Neuroscience, Eli Lilly and Company, Indianapolis, IN 46285

Protein palmitoylation is the most common posttranslational lipid modification; its reversibility mediates protein shuttling between intracellular compartments. A large family of DHHC (Asp-His-His-Cys) proteins has emerged as protein palmitoyl acyltransferases (PATs). However, mechanisms that regulate these PATs in a physiological context remain unknown. In this study, we efficiently monitored the dynamic palmitate cycling on synaptic scaffold PSD-95. We found that blocking synaptic activity rapidly induces PSD-95 palmitoylation and mediates synaptic clustering of PSD-95 and associated AMPA (α-amino-3-hydroxy-5-methyl-4-isoxazole propionic acid)-type glutamate receptors. A dendritically localized DHHC2 but not the Golgi-resident DHHC3 mediates this activity-sensitive palmitoylation. Upon activity blockade, DHHC2 translocates to the postsynaptic density to transduce this effect. These data demonstrate that individual DHHC members are differentially regulated and that dynamic recruitment of protein palmitoylation machinery enables compartmentalized regulation of protein trafficking in response to extracellular signals.

Introduction

Posttranslational modification, including phosphorylation, ubiquitination, and lipid modification, adds functional regulation to proteins beyond genomic information. Lipid modification increases protein hydrophobicity and plays a critical role in protein trafficking, targeting, and function. Thioester-linked palmitate modifies signaling proteins, enzymes, cytoskeletal proteins, ion channels, and scaffolding proteins and is involved in diverse aspects of cellular signaling (El-Husseini and Bredt, 2002; Resh, 2006; Linder and Deschenes, 2007). Recent global proteomic analyses have further expanded the known complement of palmitoylated proteins (Roth et al., 2006; Kang et al., 2008). Palmitoylation is unique in that it is a reversible modification and is proposed to be regulated by specific extracellular signals. Recent cell biological analyses revealed that some palmitoyl substrates such as small GTPases, Harvey Ras/neuroblastoma Ras (Rocks et al., 2005), and trimeric G proteins Gαo (Chisari et al., 2007)/Gαq (Tsutsumi et al., 2009) constitutively shuttle between the plasma membrane and the Golgi membrane by a palmitoylation/depalmitoylation cycle. This palmitate cycling generates and maintains the specific intracellular compartmentalization of substrates in nonpolarized cells (Rocks et al., 2006).

The postsynaptic scaffolding protein PSD-95 represents a major palmitoylated protein in neurons and plays critical roles in synaptogenesis and synaptic plasticity (Migaud et al., 1998; El-Husseini et al., 2000; Kennedy, 2000; Kim and Sheng, 2004; Funke et al., 2005). PSD-95 provides a platform for the postsynaptic clustering of crucial synaptic proteins, including AMPA (α-amino-3-hydroxy-5-methyl-4-isoxazole propionic

Correspondence to Masaki Fukata: mfukata@nips.ac.jp

Abbreviations used in this paper: 2-BP, 2-bromopalmitate; ABE, acyl-biotin exchange; AMPAR, AMPA receptor; βME, β-mercaptoethanol; CCD, charge-coupled device; CHX, cycloheximide; CM, chloroform-methanol; DIV, day in vitro; DN, dominant-negative; Kyn, kynurenic acid; LB, lysis buffer; miRNA, microRNA; NEM, N-ethyl-maleimide; NMDA, N-methyl-D-aspartate; PAT, palmitoyl acyltransferase; PPT, palmitoyl protein thioesterase; TARP, transmembrane AMPAR regulatory protein; TIRFM, total internal reflection fluorescence microscopy; TTX, tetrodotoxin; WT, wild type.

The Rockefeller University Press $30.00
J. Cell Biol. Vol. 186 No. 1 147–160
www.jcb.org/cgi/doi/10.1083/jcb.200903101

Supplemental Material can be found at:
http://jcb.rupress.org/cgi/content/full/jcb.200903101/DC1